Journal of Quantitative Spectroscopy & Radiative Transfer 110 (2009) 264–283

Contents lists available at ScienceDirect

Journal of Quantitative Spectroscopy & Radiative Transfer

journal homepage: www.elsevier.com/locate/jqsrt

$N_2(C^3\Pi_u) \rightarrow N_2(B^3\Pi_g)+h\nu$ fluorescence increase due to collisional intermolecular energy transfer induced by discharged O_2 in active nitrogen and oxygen mixtures

Efstathios Kamaratos [a,b,c,*]

[a] Physical Chemistry Sector, Department of Chemistry, University of Ioannina, GR45110 Ioannina, Greece
[b] Theoretical and Physical Chemistry Institute, National Hellenic Research Foundation, [1] 48 Vasileos Konstantinou Avenue, GR11635 Athens, Greece
[c] Department of Physics, Chemistry and Materials Technology, Technological Educational Institution of Athens,[1] Ag. Spyridonos, GR122 10 Aigaleo, Athens, Greece

ARTICLE INFO

Article history:
Received 26 June 2008
Received in revised form
3 November 2008
Accepted 10 November 2008

PACS:
31.70.Hq
34.30.+h
82.20.Hf
82.20.Pm

Keywords:
Nitrogen afterglow
Gas discharge
Nitrogen plasma
Reaction mechanisms
Kinetics
Visible and UV spectroscopy
Singlet oxygen
Photochemistry
Molecular dynamics

ABSTRACT

This work is a further investigation of increases in violet and UV fluorescence in various flowing nitrogen afterglows, when oxygen discharged in a microwave ($\mu-w$) cavity is added to active nitrogen and oxygen mixtures downstream of the $\mu-w$ discharge zones of nitrogen and oxygen. The present N_2 second positive band system (pbs) fluorescence (i.e. $N_2(C^3\Pi_u, v' \rightarrow B^3\Pi_g, v'')+h\nu$) increases also occur, when an orange flame (previously reported) is visually observed in nitrogen afterglows of active nitrogen and oxygen, by adding $\mu-w$ discharged O_2. The orange flame is reported to result from a collisional energy transfer between excited molecular oxygen and molecular nitrogen species. (Nitrogen was activated by two ways: (i) with or without argon in a $\mu-w$ discharge cavity and (ii) by reacting gaseous nitrogen with metastable argon, $Ar(^3P_{0,2})$, generated in $\mu-w$ discharged Ar.) The present, as well as previous, results indicate that the well-known metastable energy *donor*, $N_2(A^3\Sigma_u^+)$, is also an efficient energy *acceptor* from non-nitrogen species, namely from excited O_2, most probably $O_2(\alpha^1\Delta_g)$. In addition, by analyzing experimental results using two different conventional chemical kinetics approximations, a lower limit estimate ($\sim 1\times10^{-10}$ molecule^{-1} cm^3 s^{-1}) is deduced of the pseudo-unimolecular chemical reaction rate constant, $k_{\alpha A}$, for the energy transfer between $O_2(\alpha^1\Delta_g)$, as the energy donor, and $N_2(A^3\Sigma_u^+)$, as the energy acceptor. Further, enhanced intensities of background N_2^+ first negative band system (nbs) emissions (i.e. $N_2(B^2\Sigma_u^+ \rightarrow X^2\Sigma_g^+)+h\nu$) are observed along with enhanced background N_2 second pbs emissions intensities caused by discharged oxygen, near a nitrogen pink afterglow. The energy transfer, responsible for the enhanced N_2 first and second pbs emissions intensities and N_2^+ first nbs emissions intensities, may contribute to the corresponding upper atmospheric and space emissions, in particular to the various visible and UV short-lived (lasting a few to $\sim$ a thousand ms) emissions discovered since 1989, termed upper atmospheric "transient luminous events".

1. Introduction

Active nitrogen and oxygen is a research field extensively studied, the studies of which have already spanned more than 100 years [1–24]. Both, N_2 second positive band system (pbs) emissions (i.e. $N_2(C^3\Pi_u \rightarrow B^3\Pi_g)+h\nu$) and N_2^+ first negative

* Corresponding author at: Physical Chemistry Sector, Department of Chemistry, University of Ioannina, GR45110 Ioannina, Greece. Tel.: +30 210 3605863; fax: +30 210 3614625.
E-mail address: ekamarat@cc.uoi.gr
[1] Address during a sabbatical leave.

0022-4073/$ - see front matter © 2008 Elsevier Ltd. All rights reserved.
doi:10.1016/j.jqsrt.2008.11.011

band system (nbs) emissions (i.e. $N_2(B^2\Sigma_u^+ \rightarrow X^2\Sigma_g^+) + h\nu$) as well as N_2 first pbs emissions (i.e. $N_2(B^3\Pi_g \rightarrow A^3\Sigma_u^+) + h\nu$) have been observed to be constituents of emissions from nitrogen discharges, plasmas and afterglows, as well as of atmospheric emissions, in particular of the various visible and UV short-lived (lasting a few ms to ~1 s) upper atmospheric and space emissions — from colored figures of various shapes — discovered since 1989, termed upper atmospheric "transient luminous events" [8,9] and distinguished as elves, jets, giant jets, and sprites.

A large variety of processes of chemically reactive and non-reactive energy transfer occur in the abovementioned systems of active nitrogen with, or without, oxygen which give rise to formation of metastable and other excited species, as well as ground state species. Therefore, firstly, knowledge of species involved in each process and, secondly, concentrations and internal state distributions of reactants and products are required for a microscopic kinetic analysis.

In addition to the investigation of atmospheric and space natural processes [7–9,21,22], there are various applications of active nitrogen and oxygen which include environmental pollution control [23–25], material treatment [26,27], discovery of lasers [19,28–30] and biological decontamination [31].

Research work on active nitrogen and oxygen with a metal used as a catalyst in the late 1950s led to the discovery [32–36] of a red glow by mixing nitrogen atoms and discharged oxygen in a stream that was passed over the catalyst. The red glow formed as a result of enhancement of background nitrogen first pbs emissions {i.e. $N_2(B^3\Pi_g, \upsilon' \rightarrow A^3\Sigma_u^+, \upsilon'') + h\nu$} for $\upsilon' < 9$. The enhancement was initially ascribed to formation of excited NO and subsequently to N atom recombination assisted by O atoms on the catalyst that formed $N_2(A^3\Sigma_u^+)$ which, in turn, collisionally transformed into $N_2(B^3\Pi_g)$. In later work the red glow was ascribed [36] to probably excited O_2, more likely $O_2(a^1\Delta_g)$, interacting in the gas phase with $N_2(A^3\Sigma_u^+)$, or another precursor. In even later work [37], the N_2 species responsible for the red glow was postulated to be $N_2(W^3\Delta_u)$, as pointed out earlier[10], in favor of a role for $N_2(W^3\Delta_u)$, even excluding [10,13] $N_2(A^3\Sigma_u^+)$. No other [32–37] emissions, apart from N_2 first pbs emissions above ~580 nm, were reported in all of the early studies [10,32–37] on enhanced emissions from mixtures of active nitrogen and oxygen. In addition, in all of the works on the surface-catalyzed excitation of N_2, the reported red glow could not be observed unless a metal (or its oxide) and discharged oxygen were added [32–37] to the active nitrogen stream at low nitrogen pressure.

Recently, the appearance of a bright orange flame was reported [10–15] while mixing active nitrogen and active oxygen gas streams, without a catalyst, and even at much higher N_2 and O_2 pressures than ever before. The orange flame was much more intense than the background nitrogen afterglow emissions prior to the mixing of active oxygen, and was visible to the naked eye even with the laboratory lights on. It consisted [10–15] of visible N_2 first pbs emissions, even for $\upsilon' > 9$ (accompanied by IR and UV emissions), and was ascribed to collisional intersystem crossing into the $N_2(B^3\Pi_g)$ state because of interaction between excited N_2 and O_2 species (the $N_2(A^3\Sigma_u^+)$ state exclusion, in favor of the $N_2(W^3\Delta_u)$ state, was not supported by the findings, as pointed out [10, 14]). The term intersystem crossing was used not in the strict sense of singlet-triplet crossing, but in the looser more general sense of a transition even between states of the same (spin) multiplicity, however of different symmetry, used in previous work [38].

This work deals with additional enhancement [15,39] of violet-UV background nitrogen fluorescence, when discharged oxygen is added to a stream of active nitrogen and oxygen. The enhanced violet-UV background nitrogen fluorescence appears to result from several transitions from $N_2(C^3\Pi_u, \upsilon' = 0-4)$, which are part of the second pbs emissions of molecular nitrogen, $N_2(C^3\Pi_u, \upsilon') \rightarrow N_2(B^3\Pi_g, \upsilon'') + h\nu$. For the sake of complete coverage of this topic, there is an old report on enhancement of N_2 second pbs emissions intensities "over copper in an N- and O-atom stream" in the *abstract* of Ref. [34] (also cited by an anonymous referee). Nevertheless, this surface-catalyzed enhancement of N_2 second pbs emissions intensities in a stream of active nitrogen and oxygen must be due to a misprint as to the presence of oxygen, because in the text of Refs. [33,34] and in Ref. [35] the surface-catalyzed N_2 second pbs emissions intensities enhancement is reported to have been observed "in a stream of N-atoms alone" and "in active nitrogen", respectively. Therefore, the reported surface-catalyzed enhancement of N_2 second pbs emissions intensities refers to active nitrogen without discharged oxygen, actually in the absence of oxygen entirely. There is no report by other authors, to this author's knowledge, in the literature of active nitrogen and oxygen regarding enhanced N_2 second pbs afterglow emissions.

Therefore, there is a need to establish the mechanism of the observed background N_2 second pbs emissions intensities enhancements in a flowing *afterglow* of active nitrogen and active oxygen. The mechanism of N_2 band system emissions intensities enhancements may be useful in the interpretation of other phenomena as well, e.g., of the recently discovered various transient luminous events. The purpose of this work is: (i) to report further investigations of the effect of activated oxygen on nitrogen afterglow emissions that resulted in the observed violet-UV fluorescence intensities enhancements, in addition to the already reported orange flame [15]; and (ii) to interpret the observed enhancements, in order to contribute to the establishment of the energy transfer mechanism that brings them about, within the (limited) possibilities of the available experimental apparatus.

2. Experimental section

Experiments have been done to further investigate the effect of active oxygen on background N_2 second pbs emissions intensities, $N_2(C^3\Pi_u,\upsilon') \rightarrow N_2(B^3\Pi_g,\upsilon'') + h\nu$, in this work. The experimental apparatus consisted of a usual cylindrical flow reactor system. Pyrex (with, or without a quartz window) or Vycor flow tubes (of 3.4 and 4.8 cm i.d.) were used. Gaseous N_2 and O_2 were usually flowed into a Pyrex flow tube of 4.8 cm i. d. through two separate side-arms, where two 2450 MHz

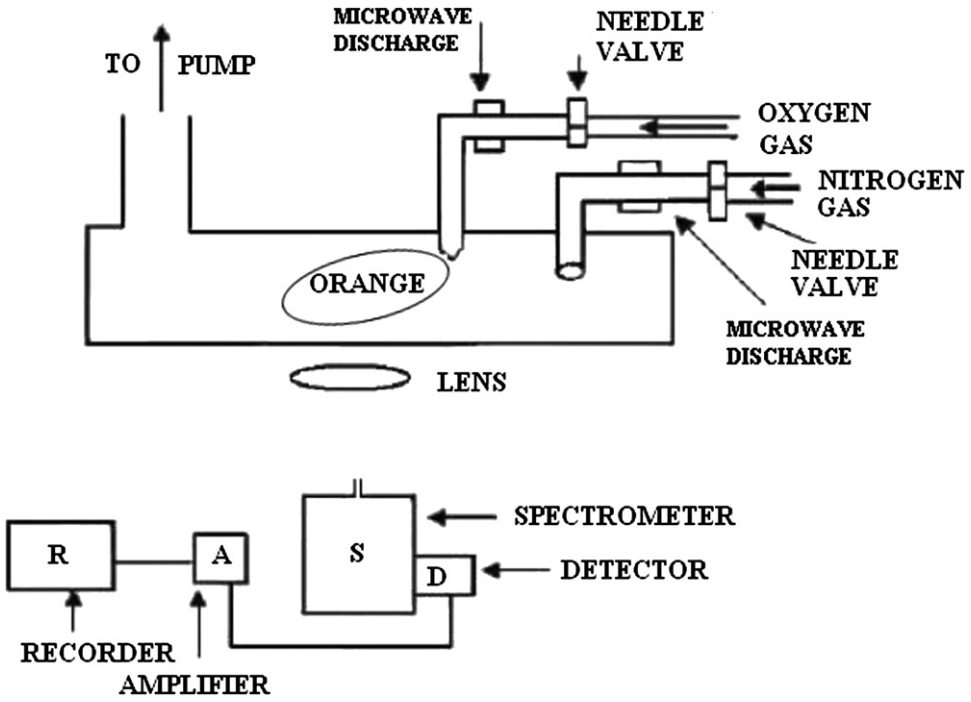

Fig. 1. A scheme of the apparatus.

microwave (μ–w) discharges could produce active nitrogen and oxygen respectively. However, some experiments were carried out with μ–w discharged mixtures of gaseous N_2 and Ar, or with mixtures of pure gaseous N_2 reacted with μ–w discharged Ar. For all conditions the distance of the injection point from the μ–w discharge in the side-arm was constant. The enhancement of N_2 second pbs emissions was observed with and without cold traps for N_2 and O_2. Observations were made normal to the flow tube with Ebert–Fastie and Czerny–Turner type spectrometers, a liquid N_2 cooled Ge photodiode detector mounted upon a trolley movable parallel to the flow tube, photomultipliers with S-20, S-5 and 605 s photocathodes and interference and color glass filters. The photomultipliers were used as detectors for the spectrometers. The Ge detector was coupled to a lock-in amplifier. The Ge photodiode was used with a narrow band interference filter (with a width at half maximum of ~2 nm around 1.27 μm) for the detection of the 1.267 μm emissions from $O_2(\alpha^1\Delta_g)$ in mixtures of nitrogen and discharged oxygen. There is no other oxygen emission in the transmission range of this filter. In preliminary experiments the Ge photodiode was used as the detector for a spectrometer with wide slits (>700 μm), in order to measure the 1.267 μm $O_2(\alpha^1\Delta_g)$ emissions from discharged oxygen alone. Gratings blazed in the first order at 600 nm and 1 μm were used. The spectra were recorded on chart recorders. The spectra in the figures are reproductions of the chart recordings. All of the reported spectra were taken in the mixing region of the active nitrogen stream with the oxygen stream. The area monitored in the mixing region corresponds to about a few ms in reaction (contact) time for low pressures, up to a few tens of ms for the higher pressures (above 10 mbar) used in the reported experiments. The distance between the μ–w discharges and the observation port was constant. The flow time for discharged nitrogen to the mixing region was estimated to be about a few tens of ms for low pressures, and a few hundreds of ms for the higher pressures (above 10 mbar) used. The spectral resolution of all reported spectra is ~0.3 nm, with the exception of those in Figs. 4 and 5, the resolution of which is ~1.0 nm. Gas flows in the range of 3–10 bar cm^3 s^{-1} were used. Fig. 1 shows a scheme of the apparatus. A longer description of the apparatus together with work on the enhancement of background nitrogen fluorescence that belongs to the first pbs emissions of N_2 appeared [10,14] recently. Special measures (e. g., use of light traps; use of black paint and/or of black cloths to blacken and/or cover parts of the flow reactor, in order to prevent stray light from reaching the observation port.) were taken as in previous work [10–15] and attention was paid to ascertain that no scattered light from the μ–w discharges and external light sources entered the spectrometer used.

3. Results

Enhancement of excited N_2 background afterglow emissions intensities was observed spectroscopically in a nitrogen afterglow of active nitrogen and active oxygen mixtures, downstream of two separate microwave discharge zones — for nitrogen, and for oxygen — in a flow reactor, in the violet and the near-UV region of the spectrum, in addition to the visible and infrared N_2 first pbs emissions previously reported [10–14], when the oxygen μ–w discharge was excited. Most of these

observed enhanced emissions intensities were identified [15] to belong to the N_2 second pbs emissions intensities, $N_2(C^3\Pi_u,\upsilon')\rightarrow N_2(B^3\Pi_g,\upsilon'')+h\nu$. Some of the bands were ascribed to N_2^+ first *nbs* emissions [1–3,40], $N_2^+(B^2\Sigma_u^+)\rightarrow N_2^+(X^2\Sigma_g^+)+h\nu$. No NO($B$–$X$) band emissions (NO β emissions) were observed under the present experimental setup, in contrast to NO(B–X) band emissions reported under a different experimental setup reported in Ref. [10]. The N_2 second pbs emissions intensities enhancement reported in this work concerns background N_2 second pbs emissions intensities in systems of nitrogen afterglows of activated nitrogen and undischarged oxygen mixtures: The background afterglow N_2 second pbs emissions intensities increase when *discharged* oxygen is added to systems of nitrogen afterglows, instead of undischarged oxygen. The emission spectra obtained in this work are presented in the following Figs. 2–8. The vibrational state quantum numbers associated with each band in a sequence are shown over each band with the $N_2(C^3\Pi_u)$ vibrational level quantum number of each band shown on top of that of the $N_2(B^3\Pi_g)$ vibrational level. The spectra are not corrected for grating and detector non uniform spectral response. The maximum absolute deviation of intensities was 10%, normally (when no great discharge instabilities occurred).

For the band intensity I to appear in a second pbs υ', υ'' emission band, $N_2(C^3\Pi_u,\upsilon')\rightarrow N_2(B^3\Pi_g,\upsilon'')+h\nu$, as a result of enhancement, it was neccessary to add discharged oxygen into a nitrogen afterglow of active nitrogen and undischarged oxygen in the flow cylindrical reactor. Active nitrogen was produced: either by subjecting N_2, with or without Ar, to a discharge excited in a $\mu-w$ cavity in a side-arm of the flow reactor, or by reacting N_2 in the flow reactor with Ar similarly $\mu-w$ discharged in the side-arm [19,24,38,41–46]. The (integrated) band intensity I is proportional to the (total) enhanced population, N, of the emitting vibronic state $N_2(C^3\Pi_u,\upsilon')$, after the background N_2 second pbs emissions intensity enhancement was brought about by $\mu-w$ discharged oxygen. The (integrated) band intensity I_o is the background N_2 second pbs emissions band intensity observed from a nitrogen afterglow in the *presence* of undischarged oxygen (with the oxygen $\mu-w$ discharge turned off). I_o is proportional to the (total) original unenhanced population, N_o, of the emitting vibronic state $N_2(C^3\Pi_u,\upsilon')$. Therefore, the enhancement ΔI in the υ', υ'' emission band (integrated) intensity is $I-I_o$, and the corresponding enhancement in the population, ΔN, of the emitting vibronic state $N_2(C^3\Pi_u,\upsilon')$ is $N-N_o$. An average relative population enhancement $\Delta N/N_o$ was determined by calculating the average value of the ratio of the emission band (integrated) intensities I/I_o only of the high enhanced and unenhanced emission band (integrated) intensities $I_{\upsilon',\upsilon''}$ and $I_{o\upsilon',\upsilon''}$ for all available υ'' corresponding to each υ'.

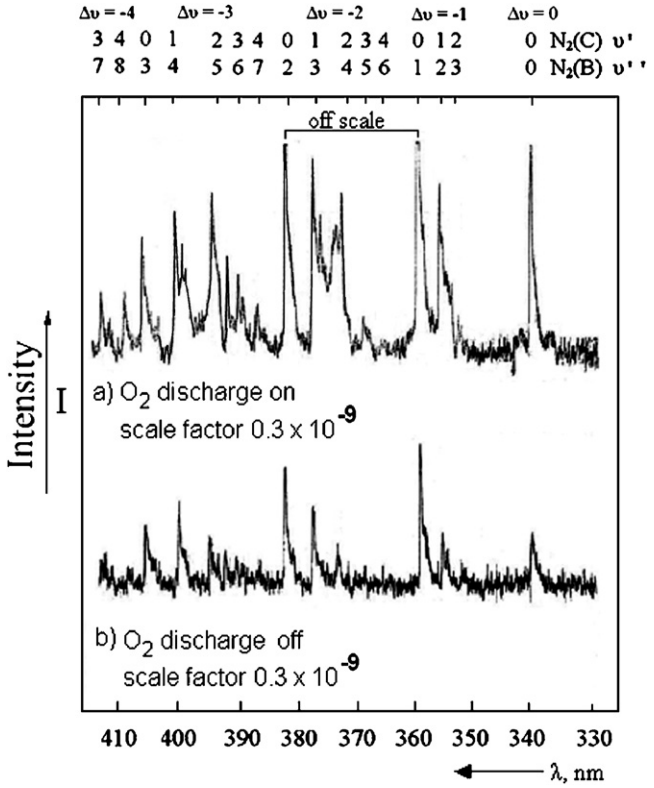

Fig. 2. The $N_2(C^3\Pi_u,\upsilon'\rightarrow B^3\Pi_g,\upsilon'')$ emission spectra with and without microwave discharged O_2 show band emission intensities from the $\Delta\upsilon=\upsilon'-\upsilon''=0$, $\Delta\upsilon=-1$, $\Delta\upsilon=-2$, $\Delta\upsilon=-3$ and $\Delta\upsilon=-4$ band sequences of the N_2 second pbs emissions. The indicated bands (0–2 and 0–1) extend off scale. Active nitrogen was generated by microwave discharging gaseous nitrogen. The top spectrum shows N_2 second pbs emissions intensity enhancement. The scale factor (here: 0.3×10^{-9}) is a multiplier also used in the rest of the figures. In both cases (a and b) $P_{N_2}=12.0$ mbar and $P_{O_2}=0.7$ mbar.

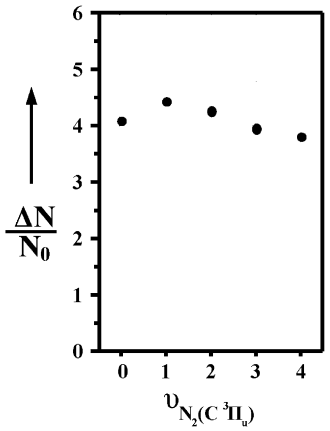

Fig. 3. Relative values of enhancement of the population, ΔN, of the emitting vibronic state $N_2(C^3\Pi_u,\upsilon')$ vs. the vibrational quantum number of the $N_2(C^3\Pi_u,\upsilon)$ vibronic state for $\upsilon = 0,1,2,3,4$. $\Delta N = N - N_o$. Active nitrogen was generated by microwave discharging gaseous nitrogen. $P_{N_2} = 10.7$ mbar and $P_{O_2} = 0.3$ mbar.

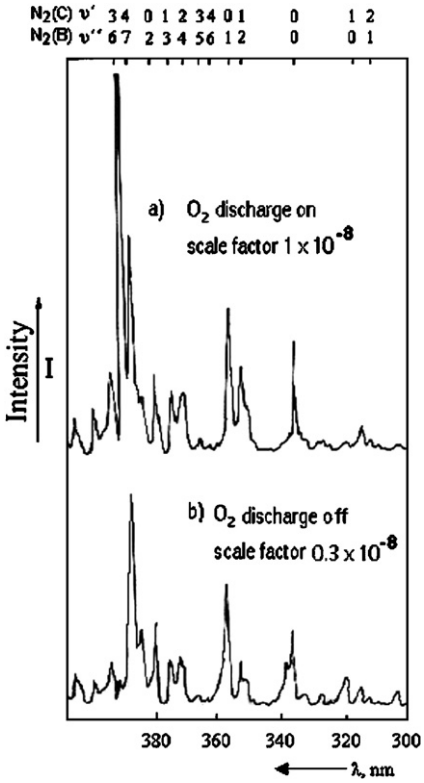

Fig. 4. The $N_2(C^3\Pi_u,\upsilon' \rightarrow B^3\Pi_g,\upsilon'')$ emission spectra, with and without microwave discharged O_2, show emission band intensities from various band sequences of the N_2 second pbs emissions, obtained by adding microwave discharged O_2 (a, top spectrum, with a scale factor of 1×10^{-8}), and undischarged O_2 (b, lower spectrum, with a scale factor of 0.3×10^{-8}) just after a flowing "pink" nitrogen afterglow extending visually downstream almost to the oxygen inlet. The top spectrum shows N_2 second pbs emissions intensity enhancement. In both cases (a and b) $P_{N_2} = 14.9$ mbar and $P_{O_2} = 1.4$ mbar.

Emission spectra from the N_2 second pbs emissions intensities reported in this research work are shown in Fig. 2 for active nitrogen with both (a) μ–w discharged oxygen and (b) undischarged oxygen. The enhancement of N_2 background emissions intensities is evident in Fig. 2a. Fig. 2a includes various enhanced emissions associated with each of all of the five vibrational quantum numbers ($\upsilon' = 0$–4) of the emitting $N_2(C^3\Pi_g,\upsilon')$ vibronic state. The enhanced N_2 second pbs emissions intensities shown in Fig. 2 are from the $\Delta\upsilon = 0$ to the $\Delta\upsilon = -4$ band sequences ($\Delta\upsilon = \upsilon' - \upsilon'' \leqslant 0$). Relative values of population enhancement $\Delta N/N_o$ as a function of the vibrational quantum number, υ', of the vibronic state $N_2(C^3\Pi_u,\upsilon')$ are shown in Fig. 3. The relative values of enhancement in the populations of the various emitting $N_2(C^3\Pi_u,\upsilon)$ vibronic states

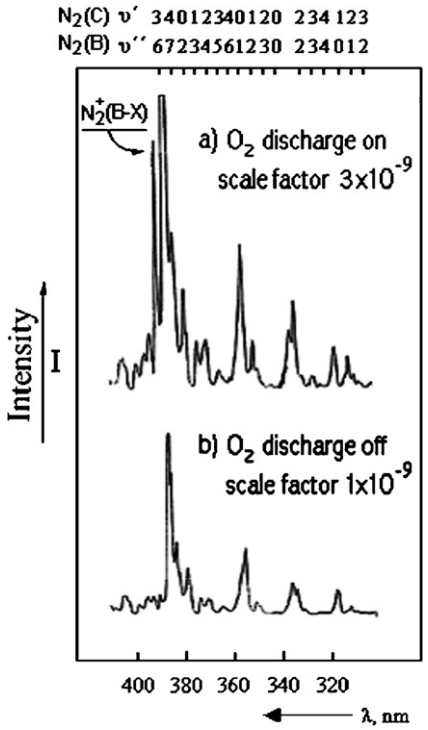

Fig. 5. The spectra show $N_2(C^3\Pi_u,v' \rightarrow B^3\Pi_g,v'')$ emission band intensities from various band sequences of the N_2 second pbs emissions, obtained as in Fig. 4. The top spectrum shows N_2 second pbs emissions intensity enhancement. In both cases (a and b) $P_{N_2} = 24.7$ mbar and $P_{O_2} = 1.2$ mbar.

were determined from the corresponding enhancement in the experimental N_2 second pbs emissions, $N_2(C^3\Pi_u,v') \rightarrow N_2(B^3\Pi_g,v'')+h\nu$, (integrated) band intensities: The experimental values of enhanced and unenhanced N_2 second pbs emissions (integrated) band intensities (i.e. integrated over the entire wavelength range of an emission band), as a function of the upper state vibrational quantum level were determined from the integrated band intensities experimentally obtained by adding discharged and undischarged oxygen to a flowing nitrogen afterglow just after a flowing "pink" nitrogen afterglow extending visually downstream almost to the oxygen inlet. The relative enhancement of the N_2 second pbs emissions intensities and of the corresponding vibronic state populations in these and other experiments [39], shown in Fig. 3, appears rather uniform within the experimental error.

Additional experiments were performed in the present work at various total pressures and compositions of nitrogen and oxygen, in order to obtain information about any pressure effects. Fig. 4 shows additional enhanced and unenhanced $N_2(C^3\Pi_u) \rightarrow N_2(B^3\Pi_g)+h\nu$ fluorescence due to collisional intermolecular energy transfer induced by $\mu-w$ discharged O_2 at higher pressures of nitrogen and oxygen in active nitrogen and oxygen mixtures, when discharged oxygen was added after the visual end of a flowing nitrogen pink afterglow extending visually downstream almost to the oxygen inlet in the cylindrical flow reactor used. Fig. 5 shows additional emission spectra from the N_2 background afterglow second pbs enhanced and unenhanced emissions at even higher pressures of active nitrogen and oxygen reported in the present research work, when discharged oxygen was added just after the visual end of a flowing nitrogen pink afterglow, just as in the case of Fig. 4.

It should be noted that the N_2^+ first nbs 0–0 band emission intensity in spectra obtained from the afterglow of active nitrogen generated by $\mu-w$ discharged N_2, and by $\mu-w$ discharged mixtures of (Ar and N_2) is enhanced when $\mu-w$ discharged O_2 is added to the active nitrogen thus formed. In a preliminary investigation of the background afterglow N_2 second pbs emissions of active nitrogen generated by reacting undischarged N_2 with $\mu-w$ discharged Ar, the 0–0 band of the N_2^+ first nbs emission, $N_2^+(B^2\Sigma_u^+) \rightarrow N_2^+(X^2\Sigma_g^+)+h\nu$, was monitored by sitting on the 391.4 nm peak. However, the N_2^+ first nbs 0–0 band emission intensity did not appear to increase when $\mu-w$ discharged O_2 was added to the active nitrogen stream in the flow reactor. It is interesting to note the dramatic increase in intensity of an emission band in the enhanced background afterglow emission spectrum in the upper part of Fig. 5 (Fig. 5a). This dramatically increased emission band at the higher pressures of nitrogen and oxygen in the active nitrogen and oxygen mixture employed in Fig. 5 was ascribed to the well-known 0–0 band of the N_2^+ first nbs emissions, $N_2^+(B^2\Sigma_u^+) \rightarrow (X^2\Sigma_g^+)$, at 391.4 nm, also mentioned in the introduction. A common feature of the spectrum both of Fig. 6 (and of Fig. 5) and of Fig. 7 is the appearance of the 0–0 emission band of the N_2^+ first nbs. In addition, the strong emissions at ~404.4 nm and ~407.6 nm appearing in Fig. 7 are tentatively ascribed to excited Ar^+, O^+, and possibly N in Discussion section.

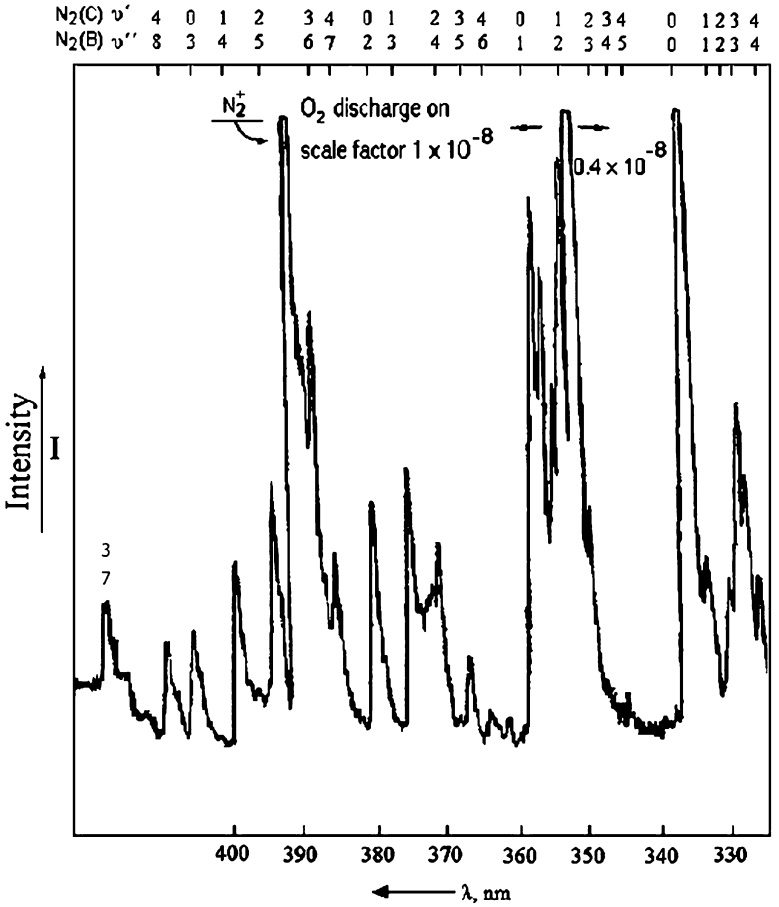

Fig. 6. An emission spectrum showing emissions intensity enhancements of various band sequences of the N_2 second pbs emissions, $N_2(C^3\Pi_u,\upsilon' \rightarrow B^3\Pi_g,\upsilon'')$. The spectrum was obtained by adding microwave discharged oxygen to a flowing nitrogen afterglow of active nitrogen produced by microwave discharging a mixture of Ar and N_2, with a scale factor of 1×10^{-8} (and partly 0.4×10^{-8}). $P_{N_2} = 1.4$ mbar, $P_{Ar} = 0.3$ mbar and $P_{O_2} = 0.2$ mbar.

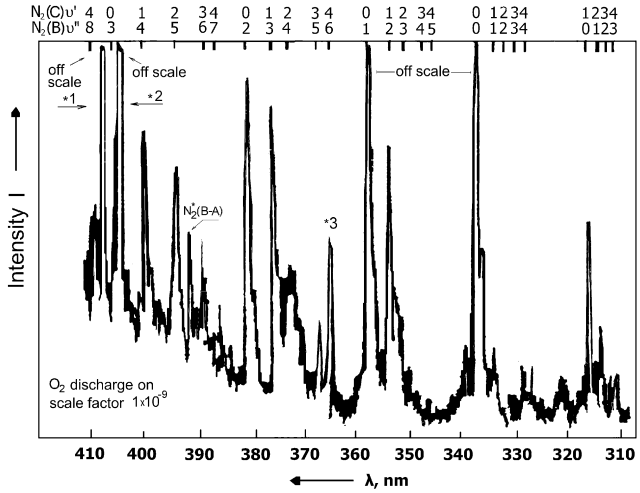

Fig. 7. An enhanced intensity emission spectrum showing various band sequences of the N_2 second pbs emissions, $N_2(C^3\Pi_u,\upsilon' \rightarrow B^3\Pi_g,\upsilon'')$. The emission spectrum was obtained by adding discharged oxygen to a flowing nitrogen afterglow of active nitrogen produced by reacting N_2 with microwave discharged Ar, with a scale factor of 1×10^{-9}. The *1 and *2 emission peaks are tentatively ascribed to emissions of excited Ar+, O+, and possibly N. The *3 emission peak (at ~365.0 nm) is tentatively ascribed to a N_2^+ first negative band system emission. $P_{N_2} = 2.0$ mbar, $P_{Ar} = 1.4$ mbar and $P_{O_2} = 0.3$ mbar.

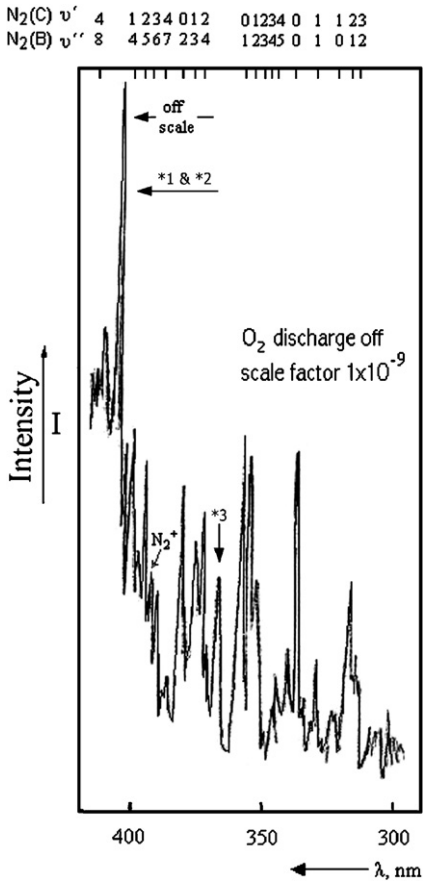

Fig. 8. An unenhanced emission spectrum showing the various band sequences of the N_2 second pbs emissions, $N_2(C^3\Pi_u,\upsilon' \rightarrow B^3\Pi_g,\upsilon'')$. The unenhanced emission spectrum was obtained by adding undischarged oxygen to a flowing nitrogen afterglow of active nitrogen produced by reacting N_2 with microwave discharged Ar, with a scale factor of 1×10^{-9}. The *1 and *2 emission peaks are tentatively ascribed to emissions of excited Ar^+, O^+, and possibly N. The *3 emission peak (at ~365.0 nm) is tentatively ascribed to a N_2^+ first negative band system emission. $P_{N_2} = 2.0$ mbar, $P_{Ar} = 1.4$ mbar and $P_{O_2} = 0.3$ mbar. The spectrum was recorded at a higher scanning rate than that in Fig. 7, that shows N_2 second pbs emissions intensity enhancements.

Some experiments were also performed with active nitrogen produced in μ–w discharged mixtures of Ar with N_2. Fig. 6 shows additional enhanced $N_2^+(C^3\Pi_u) \rightarrow N_2(B^3\Pi_g) + h\nu$ fluorescence due to collisional intermolecular energy transfer induced by discharged O_2 at much lower pressures of nitrogen, argon and oxygen in active nitrogen and oxygen. In preliminary experiments with gaseous mixtures of μ–w discharged Ar and undischarged N_2, enhancements of N_2 second pbs emissions intensities were observed by adding μ–w discharged O_2. Figs. 7 and 8 show additional enhanced and unenhanced, respectively, $N_2(C^3\Pi_u) \rightarrow N_2(B^3\Pi_g) + h\nu$ fluorescence due to collisional intermolecular energy transfer induced by μ–w discharged O_2 at lower total pressure of nitrogen, argon, and oxygen compared with the total pressures of Figs. 2–5. In the case of Figs. 7 and 8, active nitrogen was generated by reacting gaseous nitrogen with discharged gaseous argon [19,24,38,41–46].

Experiments were performed to explore the nature of the oxygen species responsible for the enhanced emissions from the $N_2(C^3\Pi_g, \upsilon')$ vibronic state: The oxygen flow was passed through a μ–w discharge and subsequently through a tube covered internally with a ring of mercuric oxide film for O atom removal [46a,b], before it entered the flow tube with a nitrogen afterglow from nitrogen discharged in a μ–w discharge. However, the N_2 second pbs emissions intensities appeared both with and without the ring of mercuric oxide film on the tube internal wall. When active oxygen was passed through glass wool for the vibrational relaxation of oxygen before its entering the flow reactor with the active nitrogen, enhancement of background N_2 afterglow emissions was still observed. In some experiments, the emission [47–51] at 1267 nm, due to the both electron spin-forbidden and angular momentum-forbidden (electric dipole moment-forbidden) radiative near-IR atmospheric transition $O_2(\alpha^1\Delta_g) \rightarrow O_2(X^3\Sigma_g^-) + h\nu$, was monitored using a Ge photodiode detector [10,11,13,14,39]. The 1.267 μm emission was observed in a cylindrical flow reactor, in which a stream of μ-w discharged oxygen was mixed with pure (undischarged) N_2. However, when the second μ-w discharge in the nitrogen side-arm was also ignited, then the 1.267 μm emission signal, from the stream of the mixture of separately μ-w discharged oxygen and nitrogen flowing in the flow reactor, was decreased. The decrease in the 1.267 μm emission signal so obtained indicates

decay of the $O_2(\alpha^1\Delta_g)$ concentration as a result of interaction of $O_2(\alpha^1\Delta_g)$ with species present in the $\mu-w$ discharged nitrogen that was mixed in the flow reactor with $\mu-w$ discharged oxygen. As in the intensities enhancement of the background N_2 first pbs emissions [10–15], the intensities enhancement of the background N_2 second pbs emissions also appears to take place by collisions between electronically excited O_2, represented hereafter as O_2^*, and some nitrogen species.

4. Discussion–interpretation

The present experiments show no O atom involvement in the N_2 second pbs emissions intensities enhancement and support the *evidence* reported in previous works [10–15] that ascribed the observed [10] enhancement of N_2 first pbs background emissions intensities to a process similar to collisional molecular intersystem excitation energy transfer to $N_2(B^3\Pi_g)$. The evidence in this, and in previous works [10–15] indicates that the most likely oxygen species responsible for the phenomenon of the intensities enhancement of the background N_2 first and second pbs emissions is the (metastable) first electronically excited state [46a–51] of O_2, $O_2(\alpha^1\Delta_g)$. The main additional reasons for the assignment of the energy donor role to $O_2(\alpha^1\Delta_g)$, in order that the background N_2 first and second pbs emissions intensities enhancement occur, are: (i) its higher lifetime (many minutes vs. seconds), (ii) its higher concentration, and (iii) its lower quenching rate compared to other electronically excited O_2 species like, e.g., $O_2(\beta^1\Sigma_g^+)$ or another O_2^* species, just as in the case of the intensities enhancement of the background N_2 first pbs emissions [10–14]. Previous research on the intensities enhancement of the background N_2 first pbs afterglow emissions [10–14] and on the chemical reaction [48,52–54] $\{O_2(\alpha^1\Delta_g)+N\}$ indicates that $O_2(\alpha^1\Delta_g)$ is quenched by atomic nitrogen very slowly, if it is at all quenched by N because of the collisional energy transfer involving $O_2(\alpha^1\Delta_g)$ and leading to the enhanced N_2 first pbs emissions which form the reported orange flame [10–14].

It is inferred which $O_2(\alpha^1\Delta_g)$ in a nitrogen afterglow is also quenched by $N_2(X^1\Sigma_g^+,\upsilon)$ very slowly, if at all by $N_2(X^1\Sigma_g^+,\upsilon)$, because of the following reasons: (i) the reported low concentration of N atoms in a nitrogen afterglow (~0.1–1%) [16a,20,52–55] and (ii) the very much higher (even by tens of times) concentration of vibrationally excited nitrogen $N_2(X^1\Sigma_g^+,\upsilon)$ in a nitrogen afterglow [56–58]. As it will be explicitly shown below, for the same extent of quenching in a unimolecular, or pseudo-unimolecular quenching reaction, the higher the concentration of the quencher, the lower the value of the quenching rate coefficient. Therefore, if it is taken into account that for a given $O_2(\alpha^1\Delta_g)$ decay in a nitrogen afterglow: (i) there is a low quenching rate coefficient, because of the low quenching rate by N atoms, if the $O_2(\alpha^1\Delta_g)$ decay is assigned to reaction with N atoms, as mentioned above; and (ii) consequently, there is an even lower quenching rate coefficient by $N_2(X^1\Sigma_g^+,\upsilon)$ molecules, if the $O_2(\alpha^1\Delta_g)$ decay is assigned to reaction with $N_2(X^1\Sigma_g^+,\upsilon)$, because of their higher concentration, at least for the low-valued υ (below $\upsilon=30$) [58], it is reasonable to draw the following conclusion:

N atoms and $N_2(X^1\Sigma_g^+,\upsilon)$ do not participate with $O_2(\alpha^1\Delta_g)$, at least directly, in the collisional energy transfer leading to the intensity enhancement of the N_2 background afterglow emissions belonging both to the first and to the second pbs emissions. Indirectly (that is, e.g., after recombination by N atoms to form some electronically excited N_2 species, represented hereafter as N_2^*, or after reaction of $N_2(X^1\Sigma_g^+,\upsilon)$ leading to another N_2^* species), of course it may be possible for enhancement both of the first and of the second pbs emissions intensities to occur by collisions with $O_2(\alpha^1\Delta_g)$.

Formation of $N_2(C^3\Pi_u)$ in a nitrogen afterglow could already in the late 1960s be explained [44,59] by the energy pooling chemical reaction of the electronically excited metastable $N_2(A^3\Sigma_u^+)$ molecules

$$N_2(A^3\Sigma_u^+)+N_2(A^3\Sigma_u^+)\rightarrow N_2(C^3\Pi_u)+N_2(X^1\Sigma_g^+). \quad (1)$$

The chemical reaction represented by Eq. (1) is the second example of an energy pooling reaction of a metastable molecule in the gas phase after that of the first electronically excited state of oxygen, the metastable molecule $O_2(\alpha^1\Delta_g)$, that generates the well-known red dimol emission at ~633.4 and at ~703.2 nm for the 0,0–0,0 and 0,0–0,1 $2O_2(\alpha^1\Delta_g)$ emissions [47,48,50], respectively.

The quadratic dependence of $N_2(C^3\Pi_u)\rightarrow N_2(B^3\Pi_g)+h\nu$ emissions intensity on the $N_2(A^3\Sigma_u^+)\rightarrow N_2(X^1\Sigma_g^+)+h\nu$ emissions (N_2 Vegard–Kaplan emissions) intensity was experimentally shown [44,59], and the overall chemical reaction rate coefficient for the pooling reaction in Eq. (1) was measured [44]. Later an almost 10 times higher value was determined both of the overall chemical reaction rate constant [60,61] for the pooling reaction in Eq. (1) and of the state specific chemical reaction rate constants[62] for the pooling reaction in Eq. (1). In the region of the nitrogen discharge the nitrogen excitation by electrons accelerated by the electromagnetic field of the incident microwaves is the prevalent process for $N_2(C^3\Pi_u)$ formation directly and, indirectly, by the collisional decay into the $N_2(C^3\Pi_u)$ state of higher metastable nitrogen energy states formed. In contrast to the discharge region, in the postdischarge region of the nitrogen afterglow the prevalent process for $N_2(C^3\Pi_u)$ formation is the energy pooling chemical reaction in Eq. (1), while the population decay (and cascading) of nitrogen higher energy states, formed by electron impact, into the $N_2(C^3\Pi_u)$ state may make a minor contribution at most: e.g., the population decay of the metastable $N_2(E^3\Sigma_g^+)$ state and, especially, of the metastable $N_2(a'^1\Sigma_u^-)$ state [6] with a longer lifetime than those of the $N_2(E^3\Sigma_g^+)$ and $N_2(w^1\Delta_u)$ states. In addition, the $N_2(a'^1\Sigma_u^-)$ and $N_2(w^1\Delta_u)$ states present [6] gateway-coupling with the $N_2(C^3\Pi_u)$ state, that results in N_2 second pbs emissions from a single characteristic vibrational-rotational level by collisions with, e.g., N_2. The emissions from each vibronic state appear in the form of a P,R line doublet. The emission spectra reported in Ref. [6] show a sharp line doublet in each emission band of the progression from the $N_2(C^3\Pi_u,\upsilon'=0,J)$ state coupled to the $N_2(a'^1\Sigma_u^-)$ state [6] and from the $N_2(C^3\Pi_u,\upsilon'=1,J)$ state

coupled to the $N_2(w^1\Delta_u)$ state. The distance between the two spectral lines in a line doublet in Fig. 2, in Ref. [6], is visually determined to be ~1 nm. The width of the line doublet is accurately determined to be slightly higher than 1.0 nm by using the spectral data in Table 1, in Ref. [6], for the reported $N_2(C^3\Pi_u,\upsilon'=0,J=14)$ coupling with the $N_2(a'\,^1\Sigma_u^-,u'=16,J=14)$ state [6]. However, there is no spike emission with a sharp line doublet in the second pbs emissions spectra in Figs. 2 and 6–8, although their spectral resolution is ~0.3 nm, certainly lower enough than 1 nm — i.e. for a spectral line to be resolved into two lines standing ~1 nm apart. (This is not the case for the spectra in Figs. 4 and 5 recorded with a resolution of ~1 nm.) It should be also noted that almost complete absence was reported [6] of gateway-induced emissions with O_2 as the collider, ascribed to the collisional quenching of the $N_2(a'\,^1\Sigma_u^-)$ state by O_2.

Therefore, a very likely candidate to interact with $O_2(\alpha^1\Delta_g)$ for the phenomenon of enhancement of the N_2 background afterglow first and second pbs emissions to occur in active nitrogen and active oxygen, when discharged oxygen is added, is the first electronically excited N_2 state, the energy-rich metastable $N_2(A^3\Sigma_u^+)$ state, in agreement with previous suggestions [12–15]. Of course, in principle, no other metastable electronically excited N_2 state can be excluded that can survive for several milliseconds in the present nitrogen afterglow and has appropriate energy to form the $N_2(C^3\Pi_u)$ state, like, e.g., the $N_2(W^3\Delta_u,\upsilon=0)$ state. Nevertheless, because the $N_2(B^3\Pi_g)$ state is efficiently quenched by [22,63–71] N_2 and by [69,71] O_2 and because the coupled N_2 triplet states are even more efficiently mixed [5,66,67,69–72] collisionally, the $N_2(W^3\Delta_u,\upsilon=0)$ state is expected to be quickly quenched — albeit, probably, by being firstly transformed to $N_2(B^3\Pi_g)$, and thus cannot participate in the reported enhancements of afterglow N_2 first and second pbs background emissions intensities by discharged O_2. In addition, the quadratic dependence of the $N_2(C^3\Pi_u)$ emissions intensity on the $N_2(A^3\Sigma_u^+)$ emissions intensity, shown experimentally [44,59,62] since the 1960s, strongly suggests the $N_2(A^3\Sigma_u^+)$ involvement [15,39] in the reported enhanced background afterglow N_2 second pbs emissions intensities.

The $N_2(A^3\Sigma_u^+)$ involvement is further supported by the intensity enhancements of N_2 background afterglow first and second pbs emissions observed also in mixtures of almost equimolar parts of discharged Ar and undischarged N_2, which have been considered a "cleaner" source of $N_2(A^3\Sigma_u^+)$ [19,24,38,41–44,62,72,73] than afterglow systems of active nitrogen generated by discharged N_2. It is well-known that the chemical reaction between N_2 and metastable Ar, $Ar(^3P_{0,2})$, transfers excitation energy to $N_2(C^3\Pi_u)$, which fast cascades to $N_2(A^3\Sigma_u^+)$ via $N_2(B^3\Pi_g)$. Fig. 7 shows such enhanced N_2 background afterglow second pbs emissions intensities The higher N_2 second pbs emissions intensities in Fig. 6 compared to those in Fig. 7 may be due to the higher $N_2(A^3\Sigma_u^+)$ concentration obtained in discharged (Ar and N_2) than in N_2 reacting with discharged Ar reported [13] in Ref. [73]. Incidentally, the pressure values for the observed N_2 background afterglow first pbs emissions enhancements reported in Figs. 7 and 8 in Ref. [14] have been interchanged, as well as the pressure values in Figs. 9 and 10 in the same reference.

The N_2^+ first nbs 0–0 band emission along with other N_2^+ first nbs emissions are key constituents of nitrogen pink afterglow emissions [1–3,40,55,74–78], of nitrogen — discharge emissions and air-discharge emissions and, in general, of nitrogen — plasma emissions and air — plasma emissions [1–3,55,79]. The lack of enhancement of the N_2^+ first nbs 0–0 band emission intensity in the afterglow of active nitrogen generated by N_2 reacting with μ–w discharged Ar, in view of its enhancement in the case of active nitrogen generated by μ–w discharged N_2, or by μ–w discharged mixtures of Ar with N_2, indicates absence or too low concentration of species involved in the energy transfer that leads to the $N_2^+(B^2\Sigma_u^+)$ excitation. If this lack of enhancement of the N_2^+ first nbs 0–0 band emission intensity is a general property of active nitrogen generated by N_2 reacting with Ar metastables, $Ar(^3P_{0,2})$, formed in μ–w discharged Ar, then it might contribute to the establishment of the species involved in the chemical reaction mechanism leading to the nitrogen pink afterglow, the mechanism of which is reported [75–77] to remain a mystery still. In any event, this contrast in enhancement of the N_2^+ first nbs 0–0 band emission intensity in the two experiments apparently confirms that the N_2^+ first nbs emission enhancement is not correlated to N_2 background afterglow second pbs emissions.

Other differences between Figs. 6 and 7 are the strong emissions at ~404.4 nm and ~407.6 nm only appearing in Fig. 7. They are tentatively ascribed to excited Ar^+, O^+, and possibly N on the basis of experimental spectral lines in Refs. [80–82]. The $O^+\{^4F(2s^22p^23d)\rightarrow{}^4D(2s^22p^23d)\}$ emission spectral lines at 407.0, 407.2, and 407.6 reported in Ref. [80] were observed in experimental studies of collisional quenching of the electronic fine structure sublevels of the $O^+\{4F(2s^22p^23d)\}$ excited state (with lifetimes of ~7 ns) produced in high energy electron impact studies [80] on gaseous O_2. The emission peak at ~365.0 nm looks rather like a (molecular) band emission, possibly due to a N_2^+ first nbs emission.

In the aforesaid preliminary experiments of nitrogen excitation by Ar μ–w discharged, the presence of the abovementioned ionic and neutral excited species' emissions in the spectrum of Fig. 7 indicates that not all excited/ionized Ar species, generated in the μ–w discharge used, were quenched/neutralized by nitrogen in the nitrogen stream before reaching the observation port.

The arguments so far presented in favor of a role for $O_2(\alpha^1\Delta_g)$ and $N_2(A^3\Sigma_u^+)$ in the enhancement of the $N_2(C^3\Pi_u)$ afterglow background emissions suggest the transfer of energy from $O_2(\alpha^1\Delta_g)$ to $N_2(A^3\Sigma_u^+)$ followed by the energy pooling chemical reaction in Eq. (1) at an accelerated rate, because of the extra internal (vibrational–rotational) excitation energy of $N_2(A^3\Sigma_u^+,\upsilon)$ transferred by $O_2(\alpha^1\Delta_g)$, as Fig. 9 suggests. Thus, the resulting higher rate of $N_2(C^3\Pi_u)$ formation by the energy pooling reaction of extra internally excited $N_2(A^3\Sigma_u^+,\upsilon)$ and the subsequent higher rate of $N_2(C^3\Pi_u)\rightarrow N_2(B^3\Pi_g)+h\nu$ emissions may account for this enhancement of the afterglow background N_2 second pbs emissions intensities in the afterglow of active nitrogen and active oxygen mixtures:

$$O_2(\alpha^1\Delta_g)+N_2(A^3\Sigma_u^+,\upsilon)\rightarrow O_2(X^3\Sigma_g^-,\upsilon'')+N_2(A^3\Sigma_u^+,\upsilon'>\upsilon). \quad (2)$$

Chemical Reactions

$$O2(\alpha\ ^1\Delta g) + N2(A\ ^3\Sigma u^+, \upsilon') \rightarrow N2(A\ ^3\Sigma u^+, \upsilon > \upsilon') + O2(X\ ^3\Sigma g^-, \upsilon'')$$

$$N2(A\ ^3\Sigma u^+, \upsilon) + N2(A\ ^3\Sigma u^+, \upsilon_A) \rightarrow N2(C\ ^3\Pi u, \upsilon_c) + N2(X\ ^1\Sigma g^+, \upsilon_x)$$

$$N2(C\ ^3\Pi u, \upsilon_c) \rightarrow N2(B\ ^3\Pi g, \upsilon_B) + h\nu$$

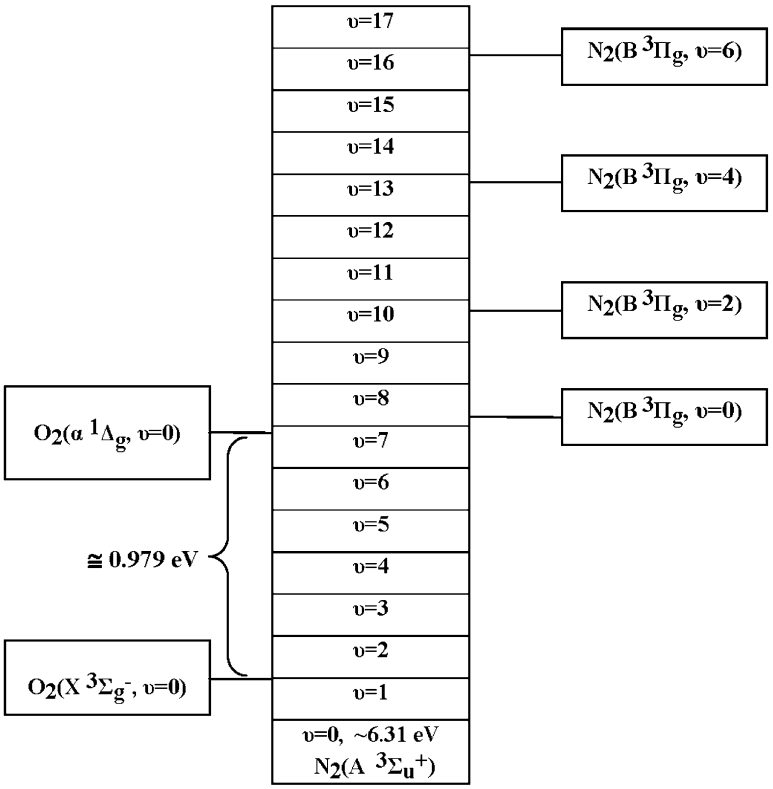

Fig. 9. A schematic diagram of vibrational energy levels of the first excited –metastable- N_2 electronic state, $N_2(A^3\Sigma_u^+)$, of the next higher N_2 electronic state, $N_2(B^3\Pi_g)$, of the first excited –metastable- O_2 electronic state, $O_2(a^1\Delta_g)$, and of the O_2 ground electronic state, $O_2(X^3\Sigma_g^-)$, with the same energy scale. The potential energy difference between $O_2(a^1\Delta_g, v' = 0)$ and $O_2(X^3\Sigma_g^-, \upsilon = 0)$ is also shown with the same energy scale. In addition, the chemical reactions are shown which are proposed to account for the background afterglow N_2 second pbs emissions intensity enhancements. The vibrational frequencies of $O_2(a^1\Delta_g)$ and $O_2(X^3\Sigma_g^-)$ are equal to 1483.5 cm^{-1} and 1580.19 cm^{-1}, respectively, while those of $N_2(A^3\Sigma_u^-)$ and $N_2(B^3\Pi_g)$ are equal to 1460.64 and 1733.39 cm^{-1}, respectively.

Arguments in favor of the energy transfer reaction $\{O_2(\alpha^1\Delta_g) + N_2(A^3\Sigma_u^+, \upsilon)\}$ were recently reported [13]. The collisional transfer of energy from $O_2(\alpha^1\Delta_g)$ to $N_2(A^3\Sigma_u^+, \upsilon)$, suggested above, can also account for the bright orange flame [10] from the enhancement of the N_2 first pbs background emissions seen in a nitrogen afterglow of active nitrogen and oxygen mixtures: the transfer of energy from $O_2(\alpha^1\Delta_g)$ to $N_2(A^3\Sigma_u^+)$ increases its internal energy content, $N_2(A^3\Sigma_u^+, \upsilon)$, in accordance with Eq. (2). $N_2(A^3\Sigma_u^+, \upsilon)$ subsequently reacts with another $N_2(A^3\Sigma_u^+)$ molecule to form $N_2((B^3\Pi_g))$ in an energy pooling chemical reaction [67,83] analogous to Eq. (1),

$$N_2(A^3\Sigma_u^+, \upsilon) + N_2(A^3\Sigma_u^+) \rightarrow N_2(B^3\Pi_g, \upsilon') + N_2(X^1\Sigma_g^+), \tag{3}$$

or, additionally, reacts with a vibrationally excited ground state N_2 molecule, $N_2(X^1\Sigma_g^+, \upsilon)$, to form [17,69,83,84] $N_2(B^3\Pi_g)$,

$$N_2(A^3\Sigma_u^+, \upsilon) + N_2(X^1\Sigma_g^+, \upsilon') \rightarrow N_2(B^3\Pi_g) + N_2(X^1\Sigma_g^+). \tag{4}$$

A large variety of atoms and molecules including the ground state oxygen molecule, $O_2(X^3\Sigma_g^-)$, were shown to convert $N_2(A^3\Sigma_u^+, \upsilon')$ into $N_2(B^3\Pi_g, \upsilon'')$ by intersystem collisional energy transfer, when $N_2(A^3\Sigma_u^+, \upsilon)$ molecules in a beam interacted with selected target molecules or rare gas atoms [4–6]. Therefore, the elementary (one-step) reaction in Eq. (5)

cannot be excluded:

$$O_2(\alpha^1\Delta_g) + N_2(A^3\Sigma_u^+, \upsilon) \rightarrow N_2(B^3\Pi_g, \upsilon'') + O_2(X^3\Sigma_g^-, \upsilon). \quad (5)$$

However, the chemical reaction in Eq. (5) might proceed only in a parallel way as a side reaction by a percentage undetermined by these experiments, but certainly not too large. Otherwise, no increased rate of formation of $N_2(C^3\Pi_g,\upsilon')$ would occur from the pooling reaction in Eq. (1) of extra internally excited $N_2(A^3\Sigma_u^+, \upsilon)$ due to energy transferred collisionally by $O_2(\alpha^1\Delta_g)$ by Eq. (2), and, consequently, no enhanced emissions from the $N_2(C^3\Pi_g,\upsilon')$ vibronic state would be observed.

This has to be so, because for each $N_2(A^3\Sigma_u^+, \upsilon)$ molecule being converted into a $N_2(B^3\Pi_g,\upsilon'')$ molecule, by the intersystem collisional energy transfer in Eq. (5), a new $N_2(A^3\Sigma_u^+, \upsilon' < \upsilon)$ molecule is formed, however mostly in a lower ($\Delta\upsilon = \upsilon - \upsilon' > 0$) or, sometimes, equal ($\Delta\upsilon = \upsilon - \upsilon' = 0$) vibrational state [1,5,17], by the subsequent $\{N_2(B^3\Pi_g, \upsilon'') \rightarrow N_2(A^3\Sigma_u^+, \upsilon') + h\nu\}$ (first pbs) emission, since a higher vibrational quantum number υ' for $N_2(A^3\Sigma_u^+, \upsilon')$ than that for $N_2(B^3\Pi_g,\upsilon'')$ is required for the $N_2(A^3\Sigma_u^+, \upsilon')$ vibronic state to closely match a $N_2(B^3\Pi_g,\upsilon'')$ vibronic state in energy for efficient collisional conversion [4–6]. The $N_2(A^3\Sigma_u^+, \upsilon' = 1)$ electronic state is lower in energy than the $N_2(B^3\Pi_g,\upsilon'' = 0)$ electronic state [1,5] by a little more than 1 eV (8065.5 cm^{-1}), while the electronic excitation energy of the metastable $O_2(\alpha^1\Delta_g,\upsilon = 0)$ state is almost 1 eV: 0.979 eV = 7894 cm^{-1}. The vibronic state $N_2(A^3\Sigma_u^+, \upsilon'' = 7)$ is slightly lower (by ~105 cm^{-1}) in energy than the $N_2(B^3\Pi_g,\upsilon' = 0)$ state, so that both can be considered to be isoenergetic with each other. The next almost isoenergetic states [1,5] are $N_2(B^3\Pi_g,\upsilon' = 2)$ and $N_2(A^3\Sigma_u^+, \upsilon'' = 10)$ by 135 cm^{-1}, $N_2(B^3\Pi_g,\upsilon' = 4)$ and $N_2(A^3\Sigma_u^+, \upsilon'' = 13)$ by 223 cm^{-1}, and $N_2(B^3\Pi_g,\upsilon' = 6)$ and $N_2(A^3\Sigma_u^+, \upsilon'' = 16)$ by 142 cm^{-1}, shown in Fig. 9.

A predominant source of $N_2^+(B^3\Sigma_u^+)$ excitation [77,78] in the nitrogen pink afterglow (as well as in a nitrogen discharge plasma because of a very much lower $N_2^+(B^2\Sigma_u^+)$ excitation rate by electron impact on $N_2^+(X^2\Sigma_g)$ and $N_2(X^1\Sigma_g^+)$) has been considered to be the ion-molecule collisions of electronic ground state N_2^+ ions with vibrationally excited N_2, according to the chemical equation

$$N_2^+(X^2\Sigma_g^+) + N_2(X^1\Sigma_g^+, \upsilon > 11) \rightarrow N_2^+(B^2\Sigma_u^+) + N_2(X^1\Sigma_g^+, \upsilon' < \upsilon). \quad (6)$$

A cross section of ~10^{-16} cm^2 was derived [78] for the excitation of $N_2^+(B^2\Sigma_u^+)$ in a nitrogen pink afterglow, in accordance with the chemical equation in Eq. (6). Generation of $N_2^+(X^2\Sigma_g^+)$ in the postdischarge region of a nitrogen discharge was suggested [77] to occur via the energy pooling chemical reactions of the metastable species $N_2(a'^1\Sigma_u^-)$ ($N_2(a'^1\Sigma_u^-)$ was misprinted as $N_2(a^1\Sigma_u^-)$ in Ref. [14]):

$$N_2(a'^1\Sigma_u^-) + N_2(a'^1\Sigma_u^-) \rightarrow N_2^+(X^2\Sigma_g^+) + N_2(X^1\Sigma_g^+) + e, \quad (7)$$

or, via the mixed metastable–metastable chemical reaction

$$N_2(A^3\Sigma_u^+) + N_2(a'^1\Sigma_u^-) \rightarrow N_2^+(X^2\Sigma_g^+) + N_2(X^1\Sigma_g^+) + e. \quad (8)$$

However, the mechanism of enhancement of the N_2^+ first nbs 0–0 band emission intensity in the afterglow of active nitrogen and oxygen is independent of the mechanism of enhancement of the N_2 second pbs emissions intensity, since enhanced background afterglow N_2 second pbs emissions intensity occur independently of the enhanced background afterglow N_2^+ first nbs 0–0 band emission intensity. More experiments are required, in order that they may shed light on the mechanism of the aforesaid enhanced afterglow N_2^+ first nbs emissions intensity.

If all of the $N_2(A^3\Sigma_u^+)$ molecules are excited via the chemical reaction in Eq. (3), then the possible maximum ratio of enhanced vs. unenhanced intensities ($I \div I_0$) of background afterglow $N_2(C^3\Pi_u) \rightarrow N_2(B^3\Pi_g) + h\nu$ (N_2 second pbs) emissions would be equal to the ratio of the rate constants for the $N_2(A^3\Sigma_u^+)$ energy pooling chemical reaction in Eq. (1) with and without the extra $N_2(A^3\Sigma_u^+)$ excitation energy transferred from $O_2(\alpha^1\Delta_g)$, respectively. Indeed, the expression for the rate of production of $N_2(C^3\Pi_u)$ (at constant reactor volume) via the elementary energy pooling chemical reaction in Eq. (1), is

$$(-1/2)d[N_2(A^3\Sigma_u^+)]/dt = d[N_2(C^3\Pi_u)]/dt = k_1[N_2(A^3\Sigma_u^+)]^2, \quad (9)$$

and the equation for the rate of the $N_2(C^3\Pi_u,\upsilon') \rightarrow N_2(B^3\Pi_g,\upsilon'') + h\nu$ vibronic emission, that is the vibronic emission intensity (radiance), I_0, is

$$I_0 = A_{\upsilon'\upsilon''}[N_2(C^3\Pi_u, \upsilon')], \quad (10)$$

where k_1 is the reaction rate constant for the elementary energy pooling chemical reaction in Eq. (9), and $A_{\upsilon'\upsilon''}$, the Einstein spontaneous emission coefficient for the $N_2(C^3\Pi_u,\upsilon' \rightarrow B^3\Pi_g,\upsilon'')$ vibronic transition in Eq. (10). However, in view of the very short lifetime [1,85] of the $N_2(C^3\Pi_u,\upsilon')$ states, the rate of $N_2(C^3\Pi_u,\upsilon')$ production equals the rate of $N_2(C^3\Pi_u,\upsilon')$ emission. Therefore, by equating the rate of $N_2(C^3\Pi_u,\upsilon')$ production with the rate of $N_2(C^3\Pi_u,\upsilon')$ destruction by emission, it is obtained:

$$I_0 = d[N_2(C^3\Pi_u)]/dt = k_1[N_2(A^3\Sigma_u^+)]^2. \quad (11)$$

The above equation holds for the case of the unenhanced intensity (I_0) of background afterglow $N_2(C^3\Pi_u) \rightarrow N_2(B^3\Pi_g) + h\nu$ emissions. A similar equation holds for the case of the enhanced intensity (I) of background afterglow N_2 second pbs

emissions, if I_0 and k_1 are replaced by I and k_1^*, respectively. Consequently

$$I/I_0 = k_1^*/k_1, \tag{12}$$

where k_1^* is the rate constant for the $N_2(A^3\Sigma_u^+, \upsilon)$ energy pooling chemical reaction in Eq. (9) with the extra $N_2(A^3\Sigma_u^+, \upsilon)$ excitation energy transferred from $O_2(\alpha^1\Delta_g)$. Nevertheless, the above possible maximum ratio of intensities only holds under the implicit assumption that the same number of $N_2(A^3\Sigma_u^+)$ molecules react via the energy pooling chemical reaction in Eq. (9) with and without the extra $N_2(A^3\Sigma_u^+)$ excitation energy transferred from $O_2(\alpha^1\Delta_g)$, respectively.

Therefore, if for some reason a number of $N_2(A^3\Sigma_u^+, \upsilon)$ molecules {with the extra $N_2(A^3\Sigma_u^+, \upsilon)$ excitation energy transferred from $O_2(\alpha^1\Delta_g)$}, that is different from the number of $N_2(A^3\Sigma_u^+)$ molecules {without the extra excitation energy transferred from $O_2(\alpha^1\Delta_g)$)}, react via the energy pooling chemical reaction in Eq. (9), then the possible maximum ratio of enhanced vs. unenhanced intensities ($I-I_0$) of background afterglow $N_2(C^3\Pi_u) \rightarrow N_2(B^3\Pi_g)+h\nu$ emissions would not be equal to the ratio of the rate constants for the $N_2(A^3\Sigma_u^+)$ energy pooling chemical reaction in Eq. (9) with and without the extra $N_2(A^3\Sigma_u^+)$ excitation energy transferred from $O_2(\alpha^1\Delta_g)$, respectively.

An estimate of $k_{\alpha A}$ was deduced [13,15] from unpublished [39,86], and (~30-year old) published data on the experimentally observed decrease in the concentration of $O_2(\alpha^1\Delta_g)$ following attempts, cited in Refs. [13,15,48,52–54,86], to determine the rate constant for the reaction $\{O_2(\alpha^1\Delta_g)+N\}$ in a nitrogen afterglow of active nitrogen and oxygen mixtures in a flow reactor. In this work a new additional estimate is also obtained from published data over the last ~35 years on the experimentally observed decrease in the concentration of $N_2(A^3\Sigma_u^+, \upsilon)$ investigated to determine the rate constant for the reactions [16,16a,21,73,87–93] $\{N_2(A^3\Sigma_u^+, \upsilon) + O(^3P)\}$ in active nitrogen and oxygen mixtures also in a flow (usually cylindrical) reactor. An estimation of the chemical reaction rate constant $k_{\alpha A}$ is shown in Appendix A.

5. Further discussion and conclusions

It is established from the $N_2(A^3\Sigma_u^+)$ pooling reactions and from corresponding isotopic nitrogen studies [4,17,68] that $N_2(A^3\Sigma_u^+)$ acts as an energy acceptor from $N_2(A^3\Sigma_u^+)$ and $N_2(X^1\Sigma_g^+, \upsilon)$, in addition to being also an energy donor towards $N_2(A^3\Sigma_u^+)$ and $N_2(X^1\Sigma_g^+, \upsilon)$, and especially to other species, as is well-known from many studies to that effect, particularly for chemical laser excitation [18,24,31], in the last ~40 years. However, it is for the first time in the observed enhancement of N_2, background (first and) second pbs emissions intensities [12–15] that $N_2(A^3\Sigma_u^+)$ is shown to act as an energy acceptor [13] from an electronically excited non-nitrogen species, O_2^*, most probably $O_2(\alpha^1\Delta_g)$. This suggested [13] new property of $N_2(A^3\Sigma_u^+)$ has a number of important ramifications in various areas of basic and applied research: e.g., in chemical kinetics and dynamics, in simulation modeling of electrical discharges and plasma emissions on the ground, and of $O(^1S)$ and triplet N_2 atmospheric and space radiation emissions in natural phenomena [8,9,21,94–98], like airglows (day- and night-glow), auroras, even the recently (as of 1989) discovered various atmospheric transient luminous events (e.g., of elves, jets and sprites) in the upper atmosphere [8,9,21,94–96]. In addition, the phenomenon of enhancement of N_2^+ and N_2 background afterglow emission intensities should also be taken into account in (upper) atmospheric emissions simulation models (e.g., for airglow, low-altitude auroral N_2 first and second pbs emissions, as well as for $O(^1S)$ upper atmospheric emissions [97,98] and for the recently discovered various atmospheric transient luminous events) [8,9,21,94–98], or anywhere such $N_2(A^3\Sigma_u^+)$ interactions with species in μ–w discharged oxygen matter. Approximately 80 years ago, the Scottish physicist C.T.R. Wilson (the Nobel laureate for the invention of the cloud chamber) predicted the appearance of flashes of light of very short duration high above large thunderstorms [99]. In point of fact, as of 1989 various reddish and bluish flashes of light lasting approximately one ms to about one thousand ms and of various shapes have been discovered [8,9,21,94–96] extending between ~30 and ~90 km in altitude, and up to many tens of km in latitude and longitude. Their spectra show N_2 first and second pbs emissions, and N_2^+ first nbs emissions [8,9,21,94–96].

The present findings about the role of O_2^* in the enhancement of N_2 background second pbs emissions are also contrary to the mechanism of $O(^3P)$ assisted N atom recombination reported [100] in earlier work [10–13], in order to interpret the enhancement of N_2 background afterglow first pbs emissions in active nitrogen and active oxygen gas mixtures. In the study of the chemical reaction [14,73], $\{N_2(A^3\Sigma_u^+, \upsilon = 0-3) + O(^3P)\}$, with exciting laser radiation from a tunable dye laser for the determination of the $\{N_2(A^3\Sigma_u^+, \upsilon = 0-3)$ concentration, a background emission was observed [73] that was presumed to originate from singlet O_2 excited in the O_2 μ-w discharge. However, experimental results also from the present investigation, in addition to those reported previously [10–14,100], show the appearance of enhanced N_2 first pbs bands, but no O_2 bands (presumed in Ref. [73] to occur), in low and high pressure emission spectra from this system. Speculative estimates of possible error up to 30% from the interaction of $N_2(A^3\Sigma_u^+)$ with $O_2(\alpha^1\Delta_g)$ in some cases were reported [24,73,91,92] for the rate constants determined for the chemical reactions $\{N_2(A^3\Sigma_u^+, \upsilon) + O(^3P)\}$. However, that interaction between $N_2(A^3\Sigma_u^+)$ and $O_2(\alpha^1\Delta_g)$ was meant to lead to actual quenching of $N_2(A^3\Sigma_u^+)$, as in the chemical reaction between $N_2(A^3\Sigma_u^+)$ and O_2. In contrast to that assumption, in the present and in the previous works [10–15] on the enhancements of N_2 background afterglow first and second pbs emissions, the available experimental evidence suggests that $N_2(A^3\Sigma_u^+)$ is excited, or converted to a more excited state, by energy transferred from $O_2(\alpha^1\Delta_g)$, as indicated in Fig. 9. In contrast to the report of no $O(^3P)$ atom production, within experimental error, in the interaction [48,53,54] of $O_2(\alpha^1\Delta_g)$ with N atoms from discharged N_2, $O(^3P)$ atom production was reported for O_2 reacting with $N_2(A^3\Sigma_u^+)$ (generated by reacting N_2 with metastable argon [19,24,73,87–89,101,102], $Ar(^3P_{0,2})$), which however is also present in discharged N_2. This, if further confirmed, indicates different behavior between $N_2(A^3\Sigma_u^+)$ and $O_2(\alpha^1\Delta_g)$, in contrast to that between $N_2(A^3\Sigma_u^+)$ and

$O_2(X^3\Sigma_g^-)$, perhaps as a result of non-reactive collisional energy transfer between them as, possibly, the N_2 first and second pbs emissions intensities enhancement.

Earlier works [91,92] on the $\{N_2(A^3\Sigma_u^+,\upsilon)+O(^3P)\}$ chemical reactions report too small a $[O_2(\alpha^1\Delta_g)]$ to be measured [92], whereas a subsequent work [73] on the aforementioned chemical reactions, under the same $[O(^3P)]$ range of up to 4×10^{12} atoms cm^{-3} and about the same N_2 pressure (within 8%), published in the same journal reports that the background emission was too large, presumably in the red singlet O_2 emissions, thus indicating a rather high $[O_2(\alpha^1\Delta_g)]$. However, in such a case, this difference in interpretation would appear to lend further support to the occurrence of the aforementioned energy transfer between $O_2(\alpha^1\Delta_g)$ and $N_2(A^3\Sigma_u^+)$, as evidenced by the enhancement of N_2 first and second pbs emissions. In any event, previous evidence and this reinterpretation of previous data on the $\{O_2(\alpha^1\Delta_g)+N\}$ and $\{N_2(A^3\Sigma_u^+,\upsilon)+O(^3P)\}$ reactions lead to an approximate estimate: $k_{\alpha A}$ is at least on the order of 10^{-10} molecule^{-1} cm^3 s^{-1}, if not gas kinetic or even larger. It should be evident that, especially since $[O(^3P)]$ is reported to be larger than $[O_2(\alpha^1\Delta_g)]$, k_o must be smaller than $k_{\alpha A}$, or else $[N_2(A^3\Sigma_u^+,\upsilon)]$ would decline, thus causing obstruction of the N_2 first and second pbs emissions enhancement.

It should be noted that the homogeneous intermolecular collisional energy transfer from $O_2(\alpha^1\Delta_g)$ to $N_2(A^3\Sigma_u^+,\upsilon)$ acts to deplete low υ $N_2(A^3\Sigma_u^+)$ state populations, in favor of those of higher υ $N_2(A^3\Sigma_u^+,\upsilon)$ states which will generate enhanced $N_2(B^3\Pi_g,\upsilon'')$ and $N_2(C^3\Pi_g,\upsilon')$ states populations. Thus, it is expected to have affected the value reported for the ratio determined of the concentrations $O(^1S)/[N_2(A^3\Sigma_u^+,\upsilon=0)]$ and, therefore, the efficiency reported [92,93] (and, consequently, the $O(^1S)$ product formation yield) of the O atom excitation reaction

$$N_2(A^3\Sigma_u^+,\upsilon)+O(^3P)\rightarrow N_2(X^1\Sigma_g^+,\upsilon')+O(^1S). \tag{13}$$

Therefore, all of the $O(^1S)$ emission simulation models (for auroras etc.) which make use of the $O(^1S)$ product formation yield of the chemical reactions in Eq. (13) need reassessment. Incidentally, the following factor in the aforesaid steady state expression for the ratio $O(^1S)/[N_2(A^3\Sigma_u^+,\upsilon=0)]$ (Eq. (10) in [92]) is erroneous. It reads: $\exp\{-\Delta k_1[O_2]+\Delta k_2[O]\}t\}$, instead of correctly reading: $\exp\{-(\Delta k_1[O]+\Delta k_2[O_2])t\}$ [14]. In order to explain the observed OI green line emissions, $\{O(^1S)\rightarrow O(^1D)+h\nu\}$, at 557.7 nm, in the upper atmospheric dayglow and nightglow (as well as in low and high altitude auroras), various theoretical models have taken into account all their well known sources (as well as the latest atmospheric parameters, such as collision cross sections, reaction rate constants and quantum yields). However, despite various readjustments by aeronomists of the value of the $O(^1S)$ product formation yield and of the laboratory values of the rate constants for the chemical reactions in Eq. (13) during the last ~25 years, these models are still unable to completely explain the experimental measurements [97,98]. Thus, before reasonable certainty can be attained in the correctness of interpretations of upper atmospheric $O(^1S)$ excitation [97,98] that leads to the OI green line emission, it will be necessary to have unchallengeable measurements of the $O(^1S)$ product formation yield, as well as of the chemical reaction rate constants for the energy transfer reactions in Eq. (13).

In addition, the fact that the abovementioned collisional energy transfer between $O_2(\alpha^1\Delta_g)$ and $N_2(A^3\Sigma_u^+,\upsilon)$ was not taken into account in the determination of the branching fraction for $NO(X^2\Pi r)$ product formation [in Eq. (1) in Ref. [102], (where all of the $N_2(A^3\Sigma_u^+,\upsilon)$ depletion chemical reactions are supposed to be included)] in the study of the chemical reactions

$$N_2(A^3\Sigma_u^+,\upsilon)+O(^3P)\rightarrow NO(X^2\Pi r)+N(^4S,^2D) \tag{14}$$

is also expected to have affected the reported values for the branching fraction for $NO(X^2\Pi r)$ product formation [102] in the study of the chemical reactions in Eq. (14) and, consequently, the reported corresponding $NO(X^2\Pi r)$ product formation yield of the aforesaid chemical reactions in Eq. (14). The effect on the reported $NO(X^2\Pi r)$ product formation yields is expected to result both, from the non-consideration [in Eq. (1) in Ref. [102] of low υ $N_2(A^3\Sigma_u^+,\upsilon)$ apparent depletion, because of the aforesaid chemical reactions $\{O_2(\alpha^1\Delta_g+N_2(A^3\Sigma_u^+,\upsilon)\}$, and from the accuracy of the determined values of the vibrational level specific bimolecular chemical reaction rate constants for the chemical reactions in Eq. (13) (used in Eq. (1) in Ref. [102]), which are expected to have been affected [13],as mentioned above because of the energy transfer between $O_2(\alpha^1\Delta_g)$ and $N_2(A^3\Sigma_u^+,\upsilon)$.

Similarly, the aforementioned energy transfer in active nitrogen and oxygen [especially between $O_2(\alpha^1\Delta_g)$ and $N_2(A^3\Sigma_u^+)$] is expected to affect observable (low υ) N_2 Vegard–Kaplan, and first and second pbs emissions, as well as N_2^+ first nbs emissions in airglows [103], in auroras [22] and in the recently discovered transient luminous events (e.g., elves, sprites, jets. The frequency of appearance of these transient luminous events may affect production of $NO(x)$ in the stratosphere, mesosphere and lower ionosphere. The production of $NO(x)$ because of the high-altitude discharges which bring about the aforesaid transient luminous events may thus have an impact on the chemistry of these atmospheric regions) [8,9,21,95,96]. E.g., because of increased energies of the primary exciting electrons auroral arcs can extend to lower altitudes in the atmosphere. There, molecular collisions with frequency sufficient for significant population redistribution may also occur. Therefore, there can be additional redistribution of the initial $N_2(A^3\Sigma_u^+)$, $N_2(B^3\Pi_g,\upsilon)$, and $N_2(C^3\Pi_g,\upsilon')$ excitation by the exciting electrons — and by cascading into the $N_2(A^3\Sigma_u^+)$ state from various N_2 triplet band systems states — caused by this homogeneous intermolecular collisional energy transfer from $O_2(\alpha^1\Delta_g)$ that increases the energy input to various N_2 triplet band systems states. This potential additional redistribution may even result in an observable change in the emitted radiation from low-altitude auroras below the critical altitude of ~100 km for molecular collisional energy

transfer to occur. Of course, this additional redistribution may not be easily distinguished from the redistribution caused by ground state molecules [5,22], like N_2 and O_2, in the low-altitude aurora, unless it is combined with other observations.

The homogeneous collisional intersystem energy transfer into $N_2(C^3\Pi_g,v)$ and $N_2(B^3\Pi_g,v')$ induced by excited O_2, as evidenced by enhancement of N_2 first and second pbs emissions in a broad range of total pressure and N_2/O_2 ratios in this and in previous works [10,12–15], remained unnoticed until recently [8] (vide below). It is expected, due to arguments in this and in previous works [10–15], to have affected several investigations [16,16a,21,22,24,32–37,53,54,73,87–92,97,98,100,102–104] adversely, and should be taken into account in all pertinent applications. $N_2(A^3\Sigma_u^+)$ appears to remain [12–15] the most likely N_2^* species to be involved in the reported enhancement of N_2 background afterglow first and second pbs emissions, contrary to earlier suggestions [37,88]. Collisional vibrational redistribution [5,22] of the triplet states $N_2(A^3\Sigma_u^+)$, $N_2(B^3\Pi_g)$ and $N_2(C^3\Pi_u)$ both by ground state molecules, as well as by $O_2(\alpha^1\Delta_g)$, should be taken into account in simulation models [8a,21,22,97,98,103,105] of pertinent excited molecular nitrogen emissions. Recently, the $\{N_2(A^3\Sigma_u^+) + O_2(\alpha^1\Delta_g) \rightarrow N_2(B^3\Pi_g) + O_2\}$ chemical reaction was considered [8] and applied [8b] in a simulation model for a sprite streamer (vide below).

The long expectation (since the 1960s) of chemical lasing, by energy transferred from $N_2(A^3\Sigma_u^+)$ to atoms or molecules (or, radicals), especially to produce a visible chemical laser, has not yet been fulfilled [106,107]. A short-wavelength (e.g., in the visible-UV range) chemical laser has been continually sought over the past ~40 years for nuclear fusion and other studies[19,24,87,106,107], mainly because of the most efficient conversion of chemical energy to laser energy and, additionally, because the lower the wavelength, the higher the absorption of radiation by materials. The phenomenon of the enhancement of N_2 background afterglow first and second pbs emissions may probably play an important role in the excitation of a laser that could be developed into a chemical laser.

In addition, the fact that the same estimate of a minimum value of $k_{\alpha A,,}$ being on the order of $\sim 1\times10^{-10}$ molecule^{-1} cm^3 s^{-1}, is obtained in the Appendix by employing the pseudo first-order approximation for the second order chemical reaction in Eq. 13, however in two different ways, gives further validity to the previous and to the present $k_{\alpha A}$ estimates and, consequently, renders the probability of a fortuitous agreement even more remote. The two different ways result by considering both: (i), $N_2(A^3\Sigma_u^+)$ to be at a steady state (that is, its concentration is practically constant) in the studies of the $O_2(\alpha^1\Delta_g)$ depletion, and (ii), $O_2(\alpha^1\Delta_g)$ to be in great excess (consequently its concentration is practically constant) in the studies of the $N_2(A^3\Sigma_u^+)$ depletion.

Following the constructive recommendations on this paper by an anonymous reviewer for this journal, the next comments were added regarding the first simulation model in which the $\{N_2(A^3\Sigma_u^+) + O_2(\alpha^1\Delta_g) \rightarrow N_2(B^3\Pi_g) + O_2\}$ chemical reaction was considered in the treatment of the N_2 first pbs emissions from a sprite in a very recent publication by Sentman et al. [8b,8c]. The results of their work [8b,8c] show that the $\{N_2(a'^1\Sigma_u^-) + N_2 \rightarrow N_2(B^3\Pi_g) + N_2\}$ chemical reaction appears to be the preponderant chemical reaction that produces $N_2(B^3\Pi_g)$ during the afterglow stage in the preliminary simulation model for a sprite streamer adopted by Sentman et al. [8b,8c], whereas the $\{N_2(A^1\Sigma_u^+) + O_2(\alpha^1\Delta_g) \rightarrow N_2(B^3\Pi_g) + O_2\}$ chemical reaction appears to play a minor role. Nevertheless, the $\{N_2(a'^1\Sigma_u^-) + N_2\}$ quenching reaction rate constant value for $N_2(B^3\Pi_g)$ formation that was employed (shown in Table A1 in the references by Sentman et al. [8b,108]) in the simulation model is a value that was implicitly assumed also in various papers on simulation studies. This value is not supported [67] by the conclusions in existing pertinent experimental publications, as reported in a recent report [109] on the paper by Sentman et al. [8b]. In addition, it is also shown in reference [109] that there are additional competing chemical reactions forming $N_2(B^3\Pi_g)$ which should be taken into account, some of which were not utilized in the simulation model adopted by Sentman et al. [8b]. So, the conclusions in Ref. [8b] regarding the role of chemical reactions leading to $N_2(B^3\Pi_g)$ formation during the afterglow stage in the simulation of a sprite streamer may very well not be definitive [109].

Acknowledgments

I acknowledge the hospitality of the late S. Spyrou, at the TPCI of HNRF, and thank Dr. N. Bacalis for his hospitality, at the TPCI of HNRF, and Prof. J. Sianoudis for his hospitality, at the TEI of Athens. I thank ΓΓΕΤ (Greek General Secretariat for Research and Technology) for the approval of a PENED 2003 grant (work 965) to continue this research, the funding from which is still pending, however, in collaboration with the TEI of Athens and NHRF. I also thank Prof. J. Sianoudis and G. Mitsou of the TEI of Athens, and the graduate students, with Prof. T. Kampanos at the University of Ioannina, G.I. Chilas and N. Kapakoglou, for assistance on drawing the figures.

Appendix A

Estimation of a chemical reaction rate constant for the $O_2(a^1\Delta_g)$ depletion via the chemical reactions:

$$O_2(a^1\Delta_g) + N_2(A^3\Sigma_u^+, v'') \rightarrow \text{Products} \quad [N_2(A^3\Sigma_u^+, v > v''), N_2(B^3\Pi_g, v'), O_2(X^3\Sigma_g^-, v''')]. \tag{A.1}$$

The equation to be used [13,15,48,61,73,91,92], in order to obtain the rate constant $k_{\alpha A}$, may be derived from the integrated rate equation for a first order (e.g., a unimolecular) chemical reaction that is also valid for a bimolecular reaction that is treated as a pseudo-first order reaction, when the concentration Q of one of the two reactants involved

remains constant:

$$C = C_o e^{-kQt}, \quad \text{or} \tag{A.2}$$

$$\ln(C/C_o) = -kQt. \tag{A.3}$$

In a flow system of mean flow velocity u and reaction (contact) time $t = z/u$ after the mixing of the two reactants, where z is the reaction distance from the mixing region of the reactants, the above equation is transformed, by substituting z/u for t, to: $u \ln(C_o/C) = kQz$, where $k = k_{\alpha A}$, C represents the varying concentration of a reactant, and C_o is C at $t = 0$, i.e. the initial reactant concentration. This equation gives k directly:

$$k = u \ln(C_o/C)/Qz. \tag{A.4}$$

However, in order to minimize the error, k is usually determined from the slope of the curve (actually of a "least squares" straight line) of the data plotted in two ways in accordance with the experimental procedure followed: C is varied either as a function of Q at a constant reaction distance (i.e. the observation point along the flow reactor remains constant), thus k is obtained from

$$k = ud \ln(C_o/C)/z \, dQ, \tag{A.5}$$

or, as a function of the reaction distance at constant Q, thus this time k is obtained from

$$k = ud \ln(C_o/C)/Q \, dz. \tag{A.6}$$

Substitution into these equations can lead to estimates of $k_{\alpha A}$. Two sets of experimental data will be next employed to determine $k_{\alpha A}$ estimates:

A.1. Data on the $O_2(\alpha^1\Delta_g)$ concentration, $[O_2(\alpha^1\Delta_g)]$, decrease

Available data [39,86] on the experimentally observed decrease in the concentration of $O_2(\alpha^1\Delta_g)$ in a nitrogen afterglow of active nitrogen and oxygen mixtures may be utilized to obtain a coarse estimate of the chemical reaction rate constant for the collisional electronic energy transfer from $O_2(\alpha^1\Delta_g)$ to $N_2(A^3\Sigma_u^+, \upsilon)$, $k_{\alpha A}$. Excited O_2 species in the metastable first electronically excited state, $O_2(\alpha^1\Delta_g)$, were generated by μ–w discharging O_2 in the presence and absence of O atoms removed either by a Hg film [46b,86], or by a HgO band [46a,46b] in the O_2 side-arm of the flow reactor, just after the discharge. The decrease in the $O_2(\alpha^1\Delta_g \rightarrow X^3\Sigma_g^-)$ 1.267 μm emission that is proportional to the $O_2(\alpha^1\Delta_g)$ concentration, $[O_2(\alpha^1\Delta_g)]$, was observed [11,86] in a nitrogen afterglow of active nitrogen and oxygen mixtures, downstream of the μ–w discharges, normal to the cylindrical flow reactor along the reaction distance with a Ge detector and a narrow band interference filter. Relative and absolute $[O_2(\alpha^1\Delta_g)]$ values were determined [86] by measuring the 1.267 μm emissions. Relative $[O_2(\alpha^1\Delta_g)]$ measurements were also made [39] by observing the red dimol oxygen emissions.

The slope of the plot of the $[O_2(\alpha^1\Delta_g)]$ logarithmic decay as a result of wall and gas phase physical deactivation vs. z, with the nitrogen discharge off, minus the slope of the same plot, however with the nitrogen discharge on, is proportional to the rate constant, k, for the $O_2(\alpha^1\Delta_g)$ quenching by species generated in and after the nitrogen discharge:

$$k = -ud \ln[C_{on}/C_{off}]/Q \, dz, \tag{A.7}$$

where C_{on}, C_{off} is the $[O_2(\alpha^1\Delta_g)]$ in the presence and absence of activated nitrogen species at constant concentration Q which quench $O_2(\alpha^1\Delta_g)$, respectively. If it is assumed that the $O_2(\alpha^1\Delta_g)$ signal attenuation is brought about by N atoms, then Q equals $[N]$, and a value of the rate constant for $O_2(\alpha^1\Delta_g)$ quenching by N atoms, $k = \sim 2 \times 10^{-15}$ molecule^{-1} cm^3 s^{-1}, is obtained for a few to several mbar of pressure of nitrogen and oxygen mixtures 40% to 60% in O_2 and for $u = \sim 80$ to ~ 200 cm s^{-1}. Relative $[N]$ was measured photometrically, being proportional to the square root of the $N_2(B^3\Pi_g, \upsilon_{high})$ emissions intensity [47]. Absolute $[N]$ ($\sim 1 \times 10^{13}$ to 4×10^{14} atoms cm^{-3}) was measured by titration with NO.

However, when it was taken into account [12,13] that $O_2(\alpha^1\Delta_g)$ appears to be mostly, if not exclusively, quenched by $N_2(A^3\Sigma_u^+)$, and very little, if at all, by N atoms (thus leading to a lower quenching rate coefficient for N atoms, k_N, and to an even less rate coefficient for the more numerous $N_2(X^1\Sigma_g^+)$ molecules, k_{N2}, as discussed under Discussion, since for the same $O_2(\alpha^1\Delta_g)$ decay it is obtained $k_N[N] = k_{N2}[N_2(X^1\Sigma_g^+)]$, as it was shown in Ref. [13]), a rough estimate of the chemical reaction rate constant for $Q = [N_2(A^3\Sigma_u^+)]$, $k_{\alpha A}$, was obtained from published data on experimentally observed concentrations of $N_2(A^3\Sigma_u^+, \upsilon)$ in a flowing nitrogen afterglow [13,15]. Indeed, more recent data from various pulsed, dc and μ-w discharges in flow systems of pure N_2 and of mixtures of N_2 and O_2 report $[N_2(A^3\Sigma_u^+, \upsilon)]$ values [16a,101,110]. A probable estimate of $[N_2(A^3\Sigma_u^+)]$ is $\sim 2 \times 10^9$ molecules cm^{-3} from Ref. [101], and gives $k_{\alpha A} \sim 1 \times 10^{-10}$ molecule^{-1} cm^3 s^{-1}. Additional estimates of $k_{\alpha A}$ on the order of $\sim 1 \times 10^{-10}$ molecule^{-1} cm^3 s^{-1} were also obtained [13,15].

A.2. Data on the $N_2(A^3\Sigma_u^+)$ concentration, $[N_2(A^3\Sigma_u^+)]$, decrease

A new, less rough estimation of $k_{\alpha A}$ may also be made from published data on the experimentally observed decrease in $[N_2(A^3\Sigma_u^+, \upsilon)]$ that was investigated, in order to determine the chemical reaction rate constant, k_o, for the chemical reactions [16,16a,24,73,87–93] $\{N_2(A^3\Sigma_u^+, \upsilon) + O(^3P)\}$ studied in active nitrogen and oxygen mixtures in a flow reactor using the

flowing afterglow technique. If $N_2(A^3\Sigma_u^+)$ reacted with $O(^3P)$ faster than with $O_2(\alpha^1\Delta_g)$ (that is, if k_o was larger than $k_{\alpha A}$), then depletion by $O(^3P)$ could inhibit the observed enhancement of N_2 background afterglow first and second pbs emissions intensities because of the aforesaid proposed $N_2(A^3\Sigma_u^+)$ involvement in the energy transfer that leads to the abovementioned N_2 background afterglow first and second pbs emissions intensities enhancement. Therefore, k_o has to be smaller than $k_{\alpha A}$, or else, depletion by $O(^3P)$ could inhibit the observed enhancement of N_2 background afterglow first and second pbs emissions intensities. The latter conclusion leads to ascribing most of the $N_2(A^3\Sigma_u^+,\upsilon)$ quenching, assigned to the chemical reaction $\{N_2(A^3\Sigma_u^+,\upsilon)+O(^3P)\}$ in previous works [16,16a,24,73,87–93], to reaction with $O_2(\alpha^1\Delta_g)$ via the chemical equations (2) and (5) under Discussion. It should also be noted that similar N_2 first and second pbs emissions intensities enhancements are observed in the presence and absence of O atoms, thus indicating that $N_2(A^3\Sigma_u^+,\upsilon)$ quenching by O is not the major $N_2(A^3\Sigma_u^+,\upsilon)$ attenuation process.

$O_2(\alpha^1\Delta_g)$ concentrations lower than that of $O(^3P)$ were reported in previous works. They might be even several times lower than $O(^3P)$ atom concentrations: e.g., a range of 20% to 60% was reported [73] for the $O(^3P)/O_2$ ratio, whereas the range of 10% to 20% was associated [73] with the $O_2(\alpha^1\Delta_g)/O_2$ ratio ($<10\%$ being more probable), in about 2 Torr of Ar with ~14 mTorr N_2, with $[O_2]$ varying up to $\sim 14\times10^{13}$ molecules cm^{-3} and $[O(^3P)]$ varying up to 10×10^{12} atoms cm^{-3}. Application of

$$k = ud\ \ln(C_o/C)/z\,dQ = -(u/z)\ \ln[C_{on}/C_{off}]/Q, \tag{A.8}$$

as above, since C_o equals $C_{off,}$ when Q equals zero, and reinterpretation of the data in Fig. 3 in Ref. [73], so that C equals $[N_2(A^3\Sigma_u^+,\upsilon)]$ and, especially, Q equals $O_2(\alpha^1\Delta_g)$, lead to an estimate of $k_{\alpha A}$ that is a multiple of the k_o value reported [73], in accordance with Eq. 3–5 in Ref. [13]:

$$k_{\alpha A} = u\,d\ln\left([N_2(A^3\Sigma u^+)]_o/[N_2(A^3\Sigma u^+)]\right)\Big/ dz[O_2(\alpha^1\Delta_g)], \tag{A.9}$$

or

$$k_{\alpha A} = \left\{u\,d\ln\left([N_2(A^3\Sigma u^+)]_o/[N_2(A^3\Sigma u^+)]\right)/dz[O(^3P)]\right\}\times\left\{[O(^3P)]/[O_2(\alpha^1\Delta_g)]\right\}, \tag{A.10}$$

or

$$k_{\alpha A} = k_0[O(^3P)]/[O_2(\alpha^1\Delta_g)]. \tag{A.11}$$

Indeed, if the ratio of $[O(^3P)]/[O_2(\alpha^1\Delta_g)]$ is 5, then $k_{\alpha A}=5k_o$. In Ref. [73], for $\upsilon=0$, k_o was reported to be equal to 3.5×10^{-11} molecule^{-1} cm^3 s^{-1}, then $k_{\alpha A}=5k_o$, or $k_{\alpha A}=1.8\times10^{-10}$ molecule^{-1} cm^3 s^{-1}. Similarly, for [73] $\upsilon=2$, a k_o value of 5.4×10^{-11} was reported, thus leading to a $k_{\alpha A}$ value: $k_{\alpha A}=5k_o=2.7\times10^{-10}$ molecule^{-1} cm^3 s^{-1}. In addition, the plot of the decay rate for the $N_2(A^3\Sigma_u^+,\upsilon=0)$ quenching in 3 Torr totally of Ar with ~10 mTorr N_2, ~0.1 to 1.0 mTorr O_2, and 0 to ~0.22 mTorr $O(^3P)$, in Fig. 3 of Ref. [90] may be reinterpreted to give an estimate of $k_{\alpha A}$ based on an estimate of the ratio $[O(^3P)]/[O_2(\alpha^1\Delta_g)]$. However, the procedure followed of passing the O_2 $\mu-w$ discharge effluents through the N_2 Tesla discharge [90] may have largely affected the $[O_2(\alpha^1\Delta_g)]$, thus introducing an additional uncertainty to other uncertainties, already reported [91], also affecting $[N_2(A^3\Sigma_u^+,\upsilon=0,1)]$. However, data in Ref. [91] regarding the $N_2(A^3\Sigma_u^+)$ attenuation may be used, instead: For the decrease in $[N_2(A^3\Sigma_u^+,\upsilon=0)]$ at 1.3 Torr Ar with (~0.2 Torr) N_2, in Ref. [91], $[O(^3P)]$ is equal up to 4×10^{12} atoms cm^{-3} and $[O_2]$ is equal to ~4x$[O(^3P)]$, that is up to $\sim1.6\times10^{13}$ molecules cm^{-3}. Then, application of $k=-(u/z)\ln[C_{on}/C_{off}]/Q$ using the value 1000 cm s^{-1} for $u\ln[C_{on}/C_{off}]$ in the plot of the $N_2(A^3\Sigma_u^+,\upsilon=0)$ decay as a function of the $[O(^3P)]$ in Fig. 2 of Ref. [91], for $z=35$ cm and for $Q=[O_2(\alpha^1\Delta_g)]$ instead of $[O(^3P)]$, as above, with the flow speed correction factor of 1.6 gives [91] an approximate value of $k_{\alpha A}$:

$$k_{\alpha A} = \sim1.6\times(1000)/\{z[O_2(\alpha^1\Delta_g)]1000\} = \sim45.7/[O_2(\alpha^1\Delta_g)]_{1000}; \tag{A.12}$$

where $[O_2(\alpha^1\Delta_g)]_{1000}$ is the value of the $[O_2(\alpha^1\Delta_g)]$ that corresponds to 1000 cm s^{-1} for u $\ln[C_{on}/C_{off}]$, which, in turn, corresponds to $[O(^3P)]$ equal to $\sim2.0\times10^{12}$ atoms cm^{-3}, as deduced from the plot in Fig. 2 of Ref. [91]. Therefore, for $[O(^3P)]$ equal to $\sim2.0\times10^{12}$ atoms cm^{-3}, and if $[O(^3P)]/[O_2(\alpha^1\Delta_g)]=5$, then $[O_2(\alpha^1\Delta_g)]_{1000}=\sim2.0\times10^{12}$ molecules $cm^{-3}/5=\sim4.0\times10^{11}$ molecules cm^{-3}. Consequently, an approximate value of $k_{\alpha A}$ is obtained: $k_{\alpha A}=\sim45.7/4.x10^{11}=\sim1.1\times10^{-10}$ molecules cm^{-3} s^{-1}.

Nevertheless, the reported chemical reaction rate constant value [91] for the chemical reaction $\{N_2A^3\Sigma_u^+,\upsilon=0)+O(^3P)\}$, $k_0=2.8\times10^{-11}$ molecule^{-1} cm^3 s^{-1}, and a subsequent estimate [92] of the ratio $[O]/[O_2(\alpha^1\Delta_g)]=\sim3.4$ associated with the obtained aforesaid k_0 value, under the same conditions of flow rate and pressure, as well as making use of Eq. (A.11) applied to the chemical reaction $\{N_2(A^3\Sigma_u^+,\upsilon=0)+O(^3P)\}$, lead to an estimate of $k_{\alpha A}=\sim3.4\times k_0=3.4\times(2.8\times10^{-11}$ molecule^{-1} cm^3 s^{-1}) $=\sim0.9(2)\times10^{-10}$ molecule^{-1} cm^3 s^{-1}

It should be noted that there has been reported [11,13,92] that the concentrations of $O_2(\alpha^1\Delta_g)$ and $O(^3P)$ are proportional under the conditions used in the studies of the chemical reaction between $N_2(A^3\Sigma_u^+)$ and $O(^3P)$. Therefore, the correlation reported [16,16a,24,73,88–93,102] between $N_2(A^3\Sigma_u^+)$ and $O(^3P)$ must also hold between $N_2(A^3\Sigma_u^+)$ and $O_2(\alpha^1\Delta_g)$ because $[O_2(\alpha^1\Delta_g)]$ is proportional to $[O(^3P)]$ under the experimental conditions employed.

It should also be noted that the above numerical replacement of the entire $[O(^3P)]$ by the $[O_2(\alpha^1\Delta_g)]$ was solely done for the sake of numerical simplification. It does in no way imply that the $\{N_2(A^3\Sigma_u^+)+O(^3P)\}$ chemical reaction does not occur as a side reaction along with the $\{O_2(a^1\Delta_g)+N_2(A^3\Sigma_u^+)\}$ chemical reaction. If the effect of the $\{N_2(A^3\Sigma_u^+)+O(^3P)\}$ side

reaction on the $N_2(A^3\Sigma_u^+)$ concentration is treated as an effective reduction in the available initial $N_2(A^3\Sigma_u^+)$ concentration, i.e. C_o that equals C_{off}, for the $\{O_2(a^1\Delta_g)+N_2(A^3\Sigma_u^+)\}$ chemical reaction, then the effective reduction in C_{off} in Eq. (A.8) in Appendix A, due to the side reaction of $N_2(A^3\Sigma_u^+\}$ with $O(^3P)\}$ leads to a smaller $k_{\alpha A}$ estimate. Therefore, as a result of the decrease in C_{off} in Eq. (A.8), the higher the extent of the course of the $\{N_2(A^3\Sigma_u^+)+O(^3P)\}$ chemical reaction, the lower the rate constant value for the $\{O_2(a^1\Delta_g)+N_2(A^3\Sigma_u^+)\}$ chemical reaction for a given amount of $N_2(A^3\Sigma_u^+)$ that reacted with oxygen species in the above experiments. However, despite the possibility of a decrease in the values of the $k_{\alpha A}$ estimates computed because of the $\{N_2(A^3\Sigma_u^+)+O(^3P)\}$ side reaction, it is a fact that all available experimental data on the $\{N_2(A^3\Sigma_u^+)+O(^3P)\}$ chemical reaction treated in Appendix A using Eqs. (A.8)–(A.12) lead to estimates of $k_{\alpha A}$ on the order of $\sim 1\times10^{-10}$ molecule^{-1} cm^3 s^{-1}. This is just the order of magnitude of all of the reasonable estimates (computed above and those already published) of $k_{\alpha A}$ based on the reinterpretation of the $\{O_2(a^1\Delta_g)+N\}$ assumed chemical reaction. Thus, the two different conventional chemical kinetics approximations (that for a steady state for $N_2(A^3\Sigma_u^+)$, as well as that for excess of $O_2(a^1\Delta_g)$) employed lead to the same estimate of $k_{\alpha A}$, something that renders the agreement among the $k_{\alpha A}$ estimates so far determined (in this work and in published works) even less fortuitous.

References

[1] Lofthus A, Krupenie PH. The spectrum of molecular nitrogen. J Phys Chem Ref Data 1977;6(1):113–307 and references therein.
[2] Anketell J, Nicholls RW. The afterglow and energy transfer mechanisms of active nitrogen. Rep Prog Phys 1970;33:269–306.
[3] Brown R, Winkler CA. The chemical behavior of active nitrogen. Angew Chem Int Edit 1970;9:181–254.
[4] Ottinger Ch, Vilesov AF, Xu DD. Isotopic study of the intermolecular versus intramolecular energy-transfer in the $N_2(W,A)$+$N_2(X)$ reactions. J Chem Phys 1995;102:1673–80 and references therein.
[5] Bachmann R, Li X, Ottinger Ch, Vilesov AF, Wulfmeyer V. J Chem Phys 1993;98:8606–26 and references therein.
[6] Ottinger Ch, Shen G. Molecular beam study of gateway-coupling $N_2(C^3\Pi_u/a'^1\Sigma_u^-)$ and chemical quenching of the metastable $N_2(a')$ state. J Chem Phys 1998;108:1997–2004 and references therein.
[7] Murad E. The shuttle glow phenomenon. Ann Rev Phys Chem 1998;49:73–95 and references therein;
[a] Kirillov AS. Electronically excited molecular nitrogen and molecular oxygen in the high-latitude upper atmosphere. Ann Geophys 2008;26:1159–69;
[b] Kirillov AS. The study of intermolecular energy transfers in electronic energy quenching for molecular collisions N_2–N_2, N_2–O_2, O_2–O_2. Ann Geophys 2008;26:1149–57.
[8] [a] Pasko VP. Red sprite discharges in the atmosphere at high altitude: The molecular physics and the similarity with laboratory discharges. Plasma Sources Sci Technol 2007;16:S13–29 and references therein;
[b] Sentman DD, Stenbaek-Nielsen HC, McHarg MG, Morrill JS. Plasma chemistry of sprite streamers. J Geophys Res 2008;113:D11112;
[c] Roussel-Dupré R, Colman JJ, Symbalisty E, Sentman D, Pasko VP. Physical processes related to discharges in planetary atmospheres. Space Sci Rev 2008;137:51–82.
[9] Williams ER. Sprites, elves, and glow discharge tubes. Phys. Today 2001;54(11):41–7.
[10] Kamaratos E. Orange flame from active nitrogen and oxygen in the absence of a metal catalyst resulting from collisional intersystem crossing into $N_2(B^3\Pi_g)$. J Phys Chem A 1997;101:2040–4 and references therein.
[11] Kamaratos E. Emissions from active nitrogen and oxygen mixtures. In: Carroll JJ, Goldman TA, editors. Proceedings of the international conference on LASERS '97. McLean, VA, USA: STS Press; 1998. p. 529–32.
[12] Kamaratos E. Energy transfer in a nitrogen afterglow in the presence of activated oxygen. Proc SPIE 2003;5131:149–57.
[13] Kamaratos E. A study of background emissions enhancements in nitrogen afterglows, due to addition of discharged O_2, in connection with the reactions $\{N_2(A^3\Sigma_u^+)+O(^3P)\}$, $\{O_2(a^1\Delta_g)+N(^4S)\}$ and $\{O_2(a^1\Delta_g)+N_2(A^3\Sigma_u^+)\}$. Cent Eur J Chem 2005;3:387–403 and references therein.
[14] Kamaratos E. Active nitrogen and oxygen: enhanced emissions and chemical reactions. Chem Phys 2006;323:271–94 and references therein.
[15] Kamaratos E. Enhanced UV emissions in active nitrogen and oxygen. Chem Phys Lett 2005;415:51–7.
[16] De Benedictis S, Dilecce G. Rate constants for deactivation of $N_2(A)$ v = 2–7 by O, O_2, and NO. J Chem Phys 1997;107:6219–29;
[a] Dilecce G, De Benedictis S. Experimental studies on elementary kinetics in N_2–O_2 pulsed discharges. Plasma Sources Sci Technol 1999;8:266–78 and references therein.
[17] Piper LG. Further observations on the nitrogen orange afterglow. J Chem Phys 1994;101:10229–36 and references therein.
[18] Cappelletti D, Liuti G, Luzzatti E, Pirani F. Characterization of a molecular beam containing metastable nitrogen and its use in scattering experiments with xenon. J Chem Phys 1994;101:1225–30 and references therein.
[19] Hewett KB, Setser DW. Chemical-kinetics of the Azide radical: rate constants for reactions with Cl; NO; NO_2; O_2; CO; CO_2; Cl_2; and C_3H_6. J Phys Chem A 1998;102:6274–81 and references therein.
[20] De Benedictis S, Dilecce G, Simek M. Excitation and decay of $N_2(B^3\Pi_g,v)$ states in a pulsed discharge: Kinetics of electrons and long-lived species. J Chem Phys 1999;110:2947–62 and references therein.
[21] Morrill JS, Bucsela E, Siefring C, Heavner M, Berg S, Moudry D, et al. Electron energy and electric field estimates in sprites derived from ionized and neutral N_2 emissions. Geophys Res Lett 2002;29(10):1462.
[22] Morrill JS, Benesch W. Auroral N_2 emissions and the effect of collisional processes on N_2 triplet state vibrational populations. J Geophys Res 1996;101:261–74 and references therein.
[23] Hueso JL, González-Elipe AR, Cotrino J, Caballero A. Plasma chemistry of NO in complex gas mixtures excited with a surfatron launcher. J Phys Chem A 2005;109:4930–8 and references therein.
[24] Herron JT. Evaluated chemical kinetics data for reactions of $N(^2D)$, $N(^2P)$ and $N_2(A^3\Sigma_u^+)$ in the gas phase. J Phys Chem Ref Data 1999;28:1453–83 and references therein.
[25] [a] Hazama M, Fujiwara H, Tanimoto M. Removal processes of nitric oxide along positive streamers observed by fluorescence imaging spectroscopy. Chem Phys Lett 2000;323:542–8;
[b] Gentile AC, Kushner MJ. Reaction chemistry and optimization of plasma remediation of N_xO_y from gas streams. J Appl Phys 1995;78:2074–85.
[26] Kato I, Noguchi K, Numada K. Preparation of silicon nitride films at room temperature using double-tubed coaxial line-type microwave plasma chemical vapor deposition system. J Appl Phys 1987;62:492–7.
[27] Ricard A, Malvos H, Bordeleau S, Hubert J. Production of active species in a common flowing post-discharge of an Ar–N_2 plasma and an Ar–H_2–CH_4 plasma. J Phys D Appl Phys 1994;27:504–8.
[28] Heard HG. Ultra-violet gas laser at room temperature. Nature 1963;16:667.
[29] Heard HG. High-power ultraviolet gas laser. Bull Am Phys Soc 1964;9:65–6.
[30] Cerny D, Bacis R, Field RW, McFarlane RA. Nitrogen $B^3\Pi_g \rightleftarrows W^3\Delta_u$ laser systems. Assignment and model for observed lasing lines. J Phys Chem 1981;85:2626–31.

[31] [a] Moreau S, Moisan M, Tabrizian M, Barbeau J, Pelletier J, Ricard A, et al. Using the flowing afterglow of a plasma to inactivate *Bacillus subtilis* spores: Influence of the operating conditions. J Appl Phys 2000;88:1166–74;
[b] Pointu AM, Ricard A, Dodet B, Odic E, Larbre J, Ganciu M. Production of active species in N_2–O_2 flowing post-discharges at atmospheric pressure for sterilization. J Phys D: Appl Phys 2005;38:1905–9 and references therein.
[32] Reeves RR, Mannella GG, Harteck P. Formation of excited NO and N_2 by wall catalysis. J Chem Phys 1960;32:946–7.
[33] Mannella GG, Reeves RR, Harteck P. Surface catalyzed excitation with N and O atoms. J Chem Phys 1960;33:63–7.
[34] Harteck P, Reeves RR, Mannella G. Surface-catalyzed atom recombinations that produce excited molecules. Can J Chem 1960;38:1648–51.
[35] Mannella GG. Active nitrogen. Chem Rev 1963;63:1–20.
[36] Weinreb MP, Mannella GG. Effect of oxygen in the surface catalyzed excitation of nitrogen. J Chem Phys 1969;51:4973–7 and references therein.
[37] Brennen W, Mc Intyre P. Vibrational relaxation and electronic mutation of metastable nitrogen molecules generated by nitrogen atom recombination on cobalt and nickel. Chem Phys Lett 1982;90:457–60.
[38] Nadler I, Setser DW, Rosenvaks S. Production of the N_2 Herman infrared system by the energy pooling reaction of $N_2(A^3\Sigma_u^+)$ metastable nitrogen molecules. Chem Phys Lett 1980;72:536–40.
[39] Kamaratos E. Unpublished data along with results cited in references 10–15 and 54.
[40] Beale Jr. GE, Broida HP. Spectral study of a visible, short-duration afterglow in nitrogen. J Chem Phys 1959;31:1030–4.
[41] Prince JF, Collins CB, Robertson WW. Spectra excited in an argon afterglow. J Chem Phys 1964;40:2619–26.
[42] Fishburne ES. Transfer of electronic energy between a metastable argon atom and a nitrogen molecule. J Chem Phys 1967;47:58–63.
[43] Meyer J A, Setser DW, Stedman DH. Excitation of the auroral green line of atomic oxygen ($^1S \rightarrow {}^1D$) by $N_2(A^3\Sigma_u^+)$. Astrophys J 1969;2:1023–5.
[44] Stedman DH, Setser DW. Energy pooling by triplet nitrogen ($A^3\Sigma_u^+$) molecules. J Chem Phys 1969;50:2256–8.
[45] Nadler I, Rosenwaks S. Studies of energy transfer processes in triplet states of N_2. I. Energy pooling by vibrationally selected $N_2(A^3\Sigma_u^+, v)$ molecules. J Chem Phys 1985;83:3932–40.
[46] Piper LG. Re-evaluation of the transition-moment function and Einstein coefficients for the $N_2(A^3\Sigma_u^+ - X^1\Sigma_g^+)$ transition. J Chem Phys 1993;99:3174–81;
[a] Bader LW, Ogryzlo EA. Reactions of $O_2(^1\Delta_g)$ and $O_2(^1\Sigma_g^+)$. Discuss Faraday Soc 1964;37:46–56;
[b] March RE, Furnival SG, Schiff H I. The production of electronically excited oxygen molecules and their reactions with ozone. Photochem Photobiol 1965;4:971–7.
[47] Kenner RD, Ogryzlo EA. Chemiluminescence in gas phase reactions. In: Burr JG, editor. Clinical and biochemical analysis, V. 16. Chemi- and bioluminescence. New York: Marcel Dekker Inc.; 1985. p. 45–186 and references therein.
[48] Wayne RP. Reactions of singlet molecular oxygen in the gas phase. In: Frimer AA, editor. Singlet O_2, vol. l, Boca Raton, LA, USA: CRC Press; 1985. p. 81–175; and references therein [chapter 4].
[49] Fink EH, Setzer KD, Wildt J, Ramsay DA, Vervloet M. Collision-induced emission of $O_2(\beta^1\Sigma_g^+ \rightarrow \alpha^1\Delta_g)$ in the gas phase. Int J Q Chem 1991;39:287–98 and references therein.
[50] Al' Dzhgami IF, Byteva IM, Gurinovich GP, Chernikov VS. Luminescence of oxygen dimolecules in the gas phase. Sov Phys Dokl 1990;35:558–60.
[51] Di Stefano G. Line-strength of the 1.27-μm atmospheric transition of oxygen. Chem. Phys 2006;323:243–8.
[52] Westenberg AA, Roscoe JM, deHaas N. Rate measurements on $N + O_2(\alpha^1\Delta_g)$ and $H + O_2(\alpha^1\Delta_g)$. Chem Phys Lett 1970;7:597–9.
[53] Clark ID, Wayne RP. Kinetics of the reaction between atomic nitrogen and molecular oxygen in the ground $O_2(X^3\Sigma_g^-)$ and first excited $O_2(\alpha^1\Delta_g)$ states. Proc R Soc London A 1970;316:539–50.
[54] Schmidt C, Schiff HI. Reactions of $O_2(^1\Delta_g)$ with atomic nitrogen and hydrogen. Chem Phys Lett 1973;23:339–42.
[55] Mi L, Xu P, Wang P-N. Temperature determination of N_2 discharge plasma by computational simulation of its emission spectra. J Phys D Appl Phys 2005;38:3885–8.
[56] Massabieaux B, Gousset G, Lefebvre M, Pe'alat M. Determination of $N_2(X)$ vibrational level populations and rotational temperatures using CARS in a D.C. low pressure discharge. J Phys 1987;48:1939–49.
[57] Supiot P, Blois D, De Benedictis S, Dilecce G, Barj M, Chapput A, et al. Excitation of $N_2(B^3\Pi_g)$ in the nitrogen short-lived afterglow. J Phys D Appl Phys 1999;32:1887–93.
[58] Loureiro J, Sa' PA, Guerra V. Role of long-lived $N_2(X^1\Sigma_g^+, \upsilon)$ molecules and $N_2(A^3\Sigma_u^+)$ and $N_2(a'^1\Sigma_u^-)$ states in the light emissions of an N_2 afterglow. J Phys D Appl Phys 2001;34:1769–78.
[59] Zipf EC. Anomalous excitation of the second positive system of nitrogen. Bull Am Phys Soc 1968;13:219.
[60] Hays GN, Oskam HJ. Reaction rate constant for $2N_2(A^3\Sigma_u^+) \rightarrow N_2(C^3\Pi_u) + N_2(X^1\Sigma_g^+, v' > 0)$. J Chem Phys 1973;59:6088–91 and references therein.
[61] Clark WG, Setser DW. Energy transfer reactions of $N_2(A^3\Sigma_u^+)$. 5. Quenching by hydrogen halides, methyl halides, and other molecules. J Phys Chem 1980;84:2225–33.
[62] Piper LG. State-to-state $N_2(A^3\Sigma_u^+)$ energy-pooling reactions. I. The formation of $N_2(C^3\Pi_u)$ and the Herman infrared system. J Chem Phys 1988;88:231–9 and references therein.
[63] Dreyer JW, Perner D. The deactivation of N_2 $B^3\Pi_g$, $v = 0$–2 and N_2 $a'^1\Sigma_u^-$, $v = 0$ by nitrogen. Chem Phys Lett 1972;16:169–73.
[64] Gartner EM, Thrush BA. Infrared emission by active nitrogen. II. The kinetic behaviour of $N_2(B^3\Pi_g)$. Proc R Soc London, Ser A 1975;346:121–37.
[65] Heidner III. RF, Sutton DG, Suchard SN. Kinetic study of $N_2(B^3\Pi_g, \upsilon)$ quenching by laser-induced fluorescence. Chem Phys Lett 1976;37:243–8.
[66] Rotem A, Rosenwaks S. Laser-induced fluorescence studies of molecular nitrogen. Opt Eng 1983;22:564–70.
[67] Piper LG. State to state $N_2(A^3\Sigma_u^+)$ energy pooling reactions II Formation and quenching of $N_2(B^3\Pi_g)$. J Chem Phys 1988;88:6911–21 and references therein.
[68] Ionikh YuZ, Chernysheva NV. Quenching of the lower vibrational levels of the B $^3\Pi_g$ state of the N_2 molecule by helium atoms. Opt Spectrosc (USSR) 1990;68:598–601.
[69] Piper LG. Energy transfer studies on $N_2(X^1\Sigma_g^+, \upsilon)$ and $N_2(B^3\Pi_g)$. J Chem Phys 1992;97:270–5.
[70] Faye A, Kou Q, Farrenq R, Picque′ N, Guelachvili G. Time-resolved Fourier transform spectroscopy applied to collisional relaxation study of the B $^3\Pi_g$ $\upsilon = 0$ level of N_2 in a pulsed electrical discharge. J Phys D Appl Phys 2002;35:2704–10.
[71] Umemoto H. Selective production and kinetic analysis of thermally equilibrated $N_2(B^3\Pi_g, v = 0)$ and $N_2(W^3\Delta_u, v = 0)$. Phys Chem Chem Phys 2003;5:5392–8.
[72] Sadeghi N, Setser DW. Collisional coupling and relaxation of $N_2(B^3\Pi_g)$ and $N_2(W^3\Delta_u)$ vibrational levels in Ar and Ne. J Chem Phys 1983;79:2710–26.
[73] Thomas JM, Kaufman F. Rate constants of the reactions of metastable $N_2(A^3\Sigma_u^+)$ in $v = 0$,1,2, and 3 with ground state O_2 and O. J Chem Phys 1985;83:2900–3.
[74] Gherman T, Eslami E, Romanini D, Kassi S, Vial J-C, Sadeghi N. High sensitivity broad-band mode-locked cavity-enhanced absorption spectroscopy: measurement of Ar* ($^3P_2$) atom and N_2^+ ion densities. J Phys D Appl Phys 2004;37:2408–15.
[75] Sá PA, Guerra V, Loureiro J, Sadeghi N. Self-consistent kinetic model of the short-lived afterglow in flowing nitrogen. J Phys D Appl Phys 2004;37:221–31.
[76] Sadeghi N. Mystery of nitrogen pink afterglow. In: Proceedings of the 27th international conference on phenomena in ionized gases, workshop in honour of Daniel Schram's 65th birthday, Eindhoven, The Netherlands, 2005. p. 1–2.
[77] Loureiro J, Sá PA, Guerra V. On the difficulty of N(^{4}S) atom recombination to explain the appearance of the pink afterglow in a N_2 flowing discharge. J Phys D Appl Phys 2006;39:122–5.
[78] Anketell J. Cross section for excitation of N_2^+ first negative bands in collisions between ground state N_2^+ ions and vibrationally excited N_2 molecules. Can J Phys 1977;55:1134–6.
[79] Yalin AP, Zare RN, Laux CO, Kruger CH. Appl Phys Lett 2002;81:1408

[80] Belikov AE, Kusnetsov OV, Sharafutdinov RG. The rate of collisional quenching of N_2O^+ ($B^2\Sigma$), N_2^+ ($B^2\Sigma$), O_2^+ ($b^4\Sigma$), O^+ (3d), O (3p), Ar^+ (4p), Ar (4p,4p) at the temperature $\leqslant$200 K. J Chem Phys 1995;102:2792–801.
[81] Moore CE, Gallagher JW, editors. Tables of spectra of atomic hydrogen, carbon, nitrogen, and oxygen atoms and ions. Boca Raton, FL: CRC Press; 1993.
[82] Vujnovic V, Wiese WL. A Critical Compilation of Atomic Transition Probabilities for Singly Ionized Argon. J. Phys. Chem. Ref. Data 1992;21:919–39.
[83] Hays GN, Oskam HJ. Population of the $N_2(B\ ^3\Pi_g)$ during the nitrogen afterglow. J. Chem. Phys. 1973;59:1507–16.
[84] Piper LG. Excitation of $N_2(B^3\Pi_g,\ v=1$–$12)$ in the reaction between $N_2(A^3\Sigma_u^+)$ and $N_2(X,v\geqslant 5)$. J Chem Phys 1989;91:864–73.
[85] Dilecce G, Ambrico PF, De Benedictis S. New $N_2(C^3\Pi_u,v)$ collision quenching and vibrational relaxation rate constants: 2. PG emission diagnostics of high-pressure discharges. Plasma Sources Sci Technol 2007;16:S45–51.
[86] Kamaratos E, Burt J, Schiff HI. Unpublished results at CRESS, York University, Toronto, Canada.
[87] Golde MF. Reactions of $N_2(A^3\Sigma_u^+)$. Int J Chem Kinet 1988;20:75–92 and references therein.
[88] Meyer JA, Setser DW, Stedman DH. Energy transfer reactions of $N_2(A^3\Sigma_u^+)$. II. Quenching and emission by oxygen and nitrogen atoms. J Phys Chem 1970;74:2238–40.
[89] Meyer JA, Setser DW, Clark G. Rate constants for quenching of molecular nitrogen ($A^3\Sigma_u^+$) in active nitrogen. J Phys Chem 1972;76:1–9.
[90] Dunn OJ, Young RA. Quenching of $N_2(A^3\Sigma_u^+)$ by O_2, O, N and H. Int J Chem Kinet 1976;8:161–72.
[91] Piper LG, Caledonia GE, Kennealy JP. Rate constants for deactivation of $N_2(A^3\Sigma_u^+\ v=0,1)$ by O. J Chem Phys 1981;75:2847–52.
[92] Piper LG. The excitation of $O(^1S)$ in the reaction between $N_2(A^3\Sigma_u^+)$ and O. J Chem Phys 1982;77:2373–7.
[93] De Souza AR, Gousset G, Touzeau M, Kheit T. Note on the determination of the efficiency of the reaction $N_2(A^3\Sigma_u^+)+O(^3P)\rightarrow N_2+O(^1S)$. J Phys B At Mol Phys 1985;18:L661–6.
[94] Su HT, Hsu RR, Chen AB, Wang YC, Hsiao WS, Lai WC, et al. Gigantic jets between a thundercloud and the ionosphere. Nature 2003;423:974–6.
[95] Pasko VP. Electric jets. Nature 2003;423:927–9.
[96] Williams E, Valente M, Gerken E, Golka R. Calibrated radiance measurements with an air-filled glow discharge tube: application to sprites in the mesosphere. Sprites, elves and intense lightning discharges. In: Füllekrug M, Mareev EA, Rycroft MJ, editors. NATO science series II: mathematics, physics and chemistry, vol. 225. Springer: Heidelberg; 2006. p. 237–51.
[97] Singh V, Upadhayaya AK. Greenline dayglow emission under equinox conditions. J Geophys Res 2004;109:A01308.
[98] Upadhayaya AK, Singh V. Effects of temperature dependence of reaction $N_2(A^3\Sigma_u^+)+O$ on greenline dayglow emission. Ann Geophys 2002;20(12):2039–45 and references therein.
[99] Wilson CTR. The electrified field of a thundercloud and some of its effects. Proc R Soc London 1925;37:32D–7D.
[100] Oldman RJ, Broida HP. Effect of oxygen and hydrogen atoms on the vibrational distribution of $N_2(B^3\Pi_g)$ in the nitrogen afterglow. J Chem Phys 1969;51:2254–8.
[101] Fraser ME, Piper LG. N_2O, $O(^3P)$, and $O_2(B^3\Sigma_u)$ product branching ratios from the $N_2(A^3\Sigma_u^+)+O_2$ reaction. J Phys Chem 1989;93:1107–11.
[102] Thomas JM, Kaufman F. An upper limit on the formation of $NO(X^2\Pi_r)$ in the reactions $N_2(A^3\Sigma_u^+)+O(^3P)$ and $N_2(A^3\Sigma_u^+)+O_2(X^3\Sigma_g^-)$ at 298 K. J Phys Chem 1996;100:8901–6.
[103] Broadfoot AL, Hatfield DB, Anderson TC, Stone TC, Sandel BR, Gardner JA, et al. N_2 triplet band systems and oxygen in the dayglow. J Geophys Res 1997;102(6):11567–84 and references therein.
[104] Morrill JS, Bucsela EJ, Pasko VP, Berg SL, Heavner MJ, Moudry DR, et al. Time resolved N_2 triplet state vibrational populations and emissions associated with red sprites. J Atmos Solar Terr Phys 1998;60:811–29.
[105] Hampton DL, Heavner MJ, Wescott EM, Sentman DD. Optical spectral characteristics of sprites. Geophys Res Lett 1996;23:89–92.
[106] APS Study Group. The science and technology of directed energy weapons. Chapter 3, Lasers. Rev. Mod. Phys. 1987;59(3):S33–67.
[107] Duo L, Tang S, Li J, Min X, Sang F, Yang B. Parametric study of $NCl(a'\ ^1\Delta)$ and $NCl(b\ ^1\Sigma)$ from the reaction of $Cl/Cl_2/He+HN_3/He$. J Phys Chem A 2002;106:743–6.
[108] Sentman DD, Stenbaek-Nielsen HC, McHarg MG, Morrill JS. Correction to "Plasma chemistry of sprite streamers". J Geophys Res 2008;113:D14399.
[109] Kamaratos E. Comment on "Plasma chemistry of sprite streamers" by D.D. Sentman, H.C. Stenbaek-Nielsen, M.G. McHarg, J.S. Morrill. J Geophys Res 2008 (accepted for publication).
[110] Sadeghi N, Foissac C, Supiot P. Kinetics of $N_2(A^3\Sigma_u^+)$ molecules and ionization mechanisms in the afterglow of a flowing N_2 microwave discharge. J Phys D Appl Phys 2001;34:1779–88.